Final Report

Research Grant 2011

Development of Automatic Expressway Incident Detection System

Sittha Jaensirisak
Agachai Sumalee
Paramet Luathep
Sakda Panwai
Saroch Boonsiripant
H.W. Ho
Jiankai Wang

Development of Automatic Expressway Incident Detection System

ASIAN TRANSPORTATION RESEARCH SOCIETY

902/1 9th Floor, Glas Haus Building, Soi Sukhumvit 25 (Daeng Prasert),
Sukhumvit Road, Klongtoey-Nua, Wattana, Bangkok 10110, Thailand
Tel. (66) 02-661-6248 FAX (66) 02-661-6249
http://www.atransociety.com

List of Members

- **Project Leader**

  Assistant Professor Dr. Sittha Jaensirisak
  Ubon Ratchathani University, Thailand

- **Project Members**

  Associate Professor Dr. Agachai Sumalee
  Hong Kong Polytechnic University, Hong Kong

  Dr. Paramet Luathep
  Prince of Songkla University, Thailand

  Dr. Sakda Panwai
  Expressway Authority of Thailand

  Dr. Saroch Boonsiripant
  Kasetsart University

  Dr. H.W. Ho
  Hong Kong Polytechnic University, Hong Kong

  Mr. Jiankai Wang
  Hong Kong Polytechnic University, Hong Kong

Table of Contents

CHAPTER 1 Introduction

1.1 Introduction

The rapid growth of many large Asian cities, such as Bangkok, have substantially increased the travel demand and resulted in serious congestions. In these congested networks, which are highly fragile due to the dense urban structure and lack of road space, one minor traffic incident could result in gridlocks and severe congestion problems. In order to efficiently and effectively handle the traffic incident for minimizing its impact to the travelers, many local authorities have investigated the possibility of implementing a traffic incident management system (TIMS). In addition, statistics showed the high chance of a more severe secondary accident following the initial accident (particularly on a high-speed highway, e.g. expressway). An ability to detect an initial accident promptly will allow the network manger to remove the incident quickly, notify the follow-up traffic of the accident ahead through VMS (to avoid the secondary accident), or even to better manage the traffic to reduce the congestion due to the accident.

The roles of TIMS are to efficiently detect the incident and then provide a series of traffic controls or information dissemination to drivers to alleviate impacts/delays caused by the incident. The main functions of TIMS could be specifically classified into three components: i) Incident detection, ii) Incident impact prediction, iii) Incident response and updating mechanism (Chang and Su, 1995; Ozbay and Kachroo, 1999; Ozbay et al., 2005; Lam, 2008). As the first step of incident management, incident detection is important in identifying the occurrence and location of traffic incident for the system operator to disseminate information and initiate contingency plan.

In the literature, data mining approaches (e.g. neural network, decision tree, Bayesian network, Kalman filter) have been adopted to devise incident detection system for urban road networks. In data mining approaches, relationships between the pattern of detector data and occurrence/location of incidents will be established based on empirical observations (Dipti et al., 2004; Chen and Wang, 2009; Wang et al., 2009; Sheu et al. 2009). Thus, the accuracy of incident detection by these approaches relies heavily on the availability/number of the traffic sensors (i.e. its spacing along a highway) and the impact of the incident (i.e. whether the incident will substantially change in traffic data collected by the detector). For cases that the traffic sensors are sparsely placed and/or the incident happens at the non-congested period, the data mining-based incident detection algorithm may not be able to detect the change of the traffic conditions for issuing an incident alarm. Some previous studies have proposed algorithms to detect incident by using image processing techniques (e.g. try to detect a non-moving object on a section of a highway) (Wu et al., 2008; Shehata et al., 2008). To deploy such a system for a wide-area network, one must install

video cameras at all key locations along the highway that demands an intensive investment on the ITS system. This is unlikely to be a feasible plan for a system in most developing countries with low budget on ITS deployment.

This project aims to develop an automatic incident detection system for an expressway system using available traffic and/or video data collected from traffic surveillance system under congested and non-congested traffic conditions. The objectives of this research are:

1. To develop a traffic parameter-based (TP-based) algorithm for incident detection on expressway with sparsely deployed detectors.
2. To develop an image processing algorithm for vehicle re-identification based on a low-resolution camera system.
3. Using (2), to develop a vehicle reidentification-based (VRI-based) algorithm for incident detection on expressway under non-congested traffic condition.
4. To test and validate the performances of the algorithms developed in (1)~(3) with case studies on an expressway system in Bangkok.
5. Based on (1)~(4), to provide recommendations for the effective implementation of the automatic expressway incident detection system

1.2 Study framework

As discussed in the previous section, incident detection is crucial in a traffic incident management system for detecting and locating the occurrence of incidents. For the situations that detectors are sparsely placed and/or the incident happens at the non-congested period, the traditional data mining approaches for incident detection have to face the problems of low detection rate and high false alarm rate. Thus, this project aims to develop an automatic incident detection system, which based on the data collected from the video-based traffic surveillance system (e.g. Autoscope), for addressing these issues.

The framework of the proposed automatic incident detection system is shown in Figure 1.1. The system will be built based on the raw video clips and traffic data (e.g. flows, occupancies, etc) collected by the video-based traffic surveillance system (Chapter 3). The traffic data will then be used by the TP-based incident detection algorithms (California algorithm, McMaster algorithm and Rule-based McMaster algorithm), which are discussed in Chapter 4, for detecting congestion-inducing incidents. On the other hand, the raw video clips will be input to the video image processing system for vehicle feature extraction (Section 5.2). The extracted vehicle feature will be used in the proposed VRI-based incident detection algorithm (Section 5.3 ~ 5.5) for detecting incident under non-congested traffic conditions. For each of the time slot, the results of incident detection from the TP-based and VRI-based incident detection algorithm will be input into a fusion

model for determining the incident status for that time slot. As the focus of this project is on the development of incident detection algorithms for different traffic conditions and sparely placed detector stations, a simple fusion model is considered (i.e. an incident alarm will be issued if either the TP-based or the VRI-based algorithm has detected an incident). Finally, the proposed incident detection algorithms in Chapter 4 and 5 will then be tested with the incident and traffic data collected in the Kanchanapisek expressway (Chapter 6).

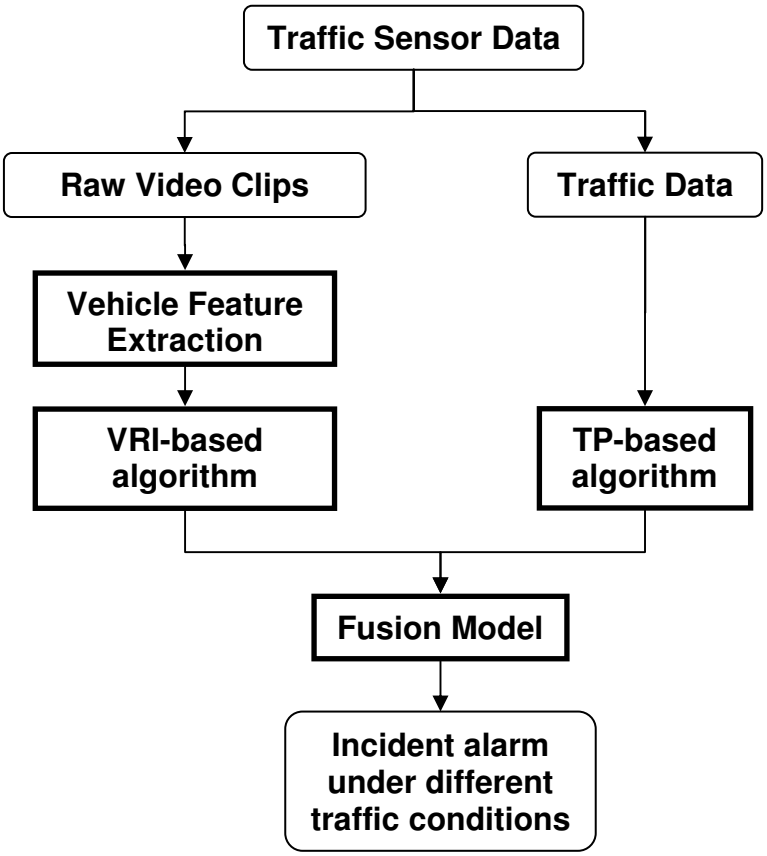

Figure 1.1 Automatic incident detection system framework.

CHAPTER 2 Literature Review

As mentioned in the previous chapter, this project is focused on developing the TP-based and VRI-based incident detection algorithm for an expressway system under different traffic conditions. Before the development of these algorithms, literatures of the traffic parameter-based approaches (Section 2.1) and vehicle re-identification approaches (Section 2.2) for incident detection are review in this chapter.

2.1 Traffic parameter-based approach for incident detection

Most existing algorithms are developed specifically for detecting incidents under heavy traffic conditions (e.g. the California algorithm series). The assumption behind these algorithms is that the traffic parameters (e.g. travel time, traffic flow, traffic delay, etc) will change dramatically as incidents occur under congested traffic. Generally, these algorithms can be divided into four different groups: 1) comparative algorithms; 2) statistical algorithms (e.g. Bayesian networks); 3) filtering algorithms; and 4) dynamic traffic modeling algorithm. Owing to the worldwide deployment of inductive loop sensors, most studies have focused on detecting incidents using data collected from loop detectors. Nevertheless, other algorithms (e.g. image processing method) have also considered the using of data from emerging traffic surveillance technologies.

Owing to their computational and theoretical simplicity, California algorithms (Payne and Thompson, 1997, Payne and Tignor, 1978) are the most widely adopted comparative algorithms. The underlying principle of the California algorithms is that incident would normally result in a substantial increase in the upstream occupancy while simultaneously reducing the downstream one. Thus, a direct comparison between the upstream and downstream occupancy data obtained from consecutive loop detectors would help to determine the occurrence of incident. In these algorithms, incident alarm will be prompted if the differences between the occupancies exceed the established thresholds. In order to reduce the false alarm rate, the decision tree approach, with different measures of occupancy difference (e.g. absolute or relative difference of occupancy between upstream and downstream detectors), are introduced for issuing incident alarm (Payne and Tignor, 1978). It is obvious that the success of these comparative algorithms is heavily dependent on the accuracy of traffic sensors in measuring traffic parameters. As it is unavoidable that traffic data contain potential noise, especially under the congested traffic conditions, the accuracy of these algorithms will be seriously affect.

To compensate the deficiency of comparative algorithms under congested traffic condition, statistical algorithms for incident detection are proposed. These approaches apply standard

statistical technique to determine whether the collected traffic parameters (e.g. flow, occupancy, travel time, etc) are statistically different from the estimated parameters. Levin and Krause (1978) has utilized Bayesian statistics to compute the likelihood of having an incident based on the historical databases of incident and incident-free traffic conditions. Within the Bayesian framework, it is assumed that the collected traffic data are random variables and follow certain statistical distributions. Apart from the randomly defined traffic data, prior knowledge (prior distribution) of the likelihood that an incident has happened is also defined based on the historical database. With the Bayesian update on the prior distribution, a posterior probability regarding the likelihood of having an incident at the evaluation time could be obtained. In Levin and Krause (1978), these posterior probabilities, which come from different measures of the collected traffic parameters, are applied to the decision tree approach for reducing the false alarm rate. Similar Bayesian based incident detection algorithm could also be found in Zhang and Taylor (2006).

Filtering algorithms (Stephanedes and Chassiakos, 1993a,b) are also designed to remove the noise from the collected traffic data. As opposed to the use of statistical model in representing the uncertainties of traffic data, these filtering algorithms use the typical filters (e.g. low-pass filter, Kalman filter) to directly eliminate the noises from the collected data. After the filtering process, comparative algorithms (e.g. California algorothms) are adopted to determine the occurrence of incidents.

The accuracy of the aforementioned algorithms relies on the availability and diversity of incident data, which requires a dense deployment of traffic sensors over the network. Besides, these approaches also fail to consider the temporal evolution and temporal/spatial correlation of the collected traffic data. In order to overcome these difficulties, several studies have focused on the development of dynamic traffic models for incident detection (Balke et al., 2007, Lee and Taylor, 1999, Willsky et al., 1980). These algorithms utilize the dynamic traffic flow models (e.g. queue model, cell transmission model) to capture the dynamic nature of traffic and to estimate the traffic parameters (e.g. travel time, speed, traffic flow). By comparing the estimated and measured traffic parameters, abrupt changes could be identified in real time, and, thus, occurrence of incident could be detected.

2.2 Vehicle re-identification approach for incident detection

Detecting incidents under free flow, or non-congested, condition is difficult as it faces the following two major challenges. First, the conventional traffic sensors (i.e. inductive loops) are not able to provide traffic data with satisfactory quality under free flow condition. Due to the limitation of the sampling rate of inductive loops, the individual vehicle data (e.g. vehicle speed, vehicle length) cannot be collected accurately if a vehicle is travelling at high speed (Coifman and Krishnamurthy, 2007). Such inaccurate traffic data causes a serious problem for developing the traditional data

mining based incident detection algorithm. Second, under the free flow condition, a drop in traffic capacity due to an incident (e.g. one lane blocking) may not cause any traffic delay or change in flow pattern. Therefore, it is not feasible to detect the incident through analyzing the macroscopic traffic parameters. To handle the aforementioned challenges, Shehata et al. (2008) conducted a study to detect the incident by identifying non-moving vehicles (i.e. caused by an incident) from video records by using image processing techniques. Although this method appears to be theoretically sound, the deployment of such system requires the installation of cameras at all key locations along the expressways, which is not practically feasible for monitoring a wide-area network. In this case, the approaches that focus on the continuous tracking of individual vehicles across consecutive detectors provide a promising way for incident detection. The rationale behind this idea is straightforward. For a closed expressway system, if one can track all the vehicles along the designated points, a disappearance of any vehicle movement between consecutive points can be classified as a potential incident. Based on this principle, Farmbro and Ritch (1980) designed a "vehicle count approach" to trace and identify the "missing" vehicle through the vehicle count data obtained from the loop detectors. Given the vehicle speed at upstream, the arrival time window at downstream could be estimated. By comparing the vehicle counts in this arrival time window with the corresponding counts in the upstream, one may be able to identify the missing vehicle (if any) for incident detection. However, the performance of this approach is largely dependent on the accuracy of the vehicle count data and the estimated arrival time window. Owing to the unreliable traffic data collected by loop sensors under free flow condition, false alarms may be triggered. Also, the overlapping of arrival time windows of different vehicles would lead to a significant increase in the detection time (This will be discussed in more detail in Section 5.3.1).

To further reduce the incident detection time, much attention has been paid to track the vehicle by utilizing the emerging automatic vehicle identification (AVI) systems: automatic number plate recognition (Chang et al., 2004), or Bluetooth identification technology (Quayle et al., 2010). Although the AVI technologies enable a more efficient tracking of vehicles across multiple points by accurately matching their unique identity (e.g. plate number, media access control address), the installation of these systems is expensive and may raise privacy issues. In this case, the vehicle re-identification (VRI) scheme, which does not intrude driver's privacy, provides a tool to devise a more practical and effective incident detection algorithm under free flow condition. Generally, vehicle re-identification is a process of matching vehicle signature (e.g. waveform, vehicle length, etc) from one detector to the next one in the traffic network. The non-uniqueness of the vehicle signature would allow the VRI system to track the vehicle anonymously. During the past few years, extensive researches were carried out to develop VRI systems based on conventional loop detectors (e.g. Coifman and Cassidy, 2002; Coifman, 1998; Sun et al., 1999). As explained previously, the unreliability of the loop detectors under free flow condition may compromise the performance (i.e. matching accuracy) of these VRI systems. Recently, Sumalee and Wang (2012) developed a VRI system by utilizing the emerging video image processing systems. Various

detailed vehicle features (e.g. vehicle color, length and type) were extracted and a probabilistic data fusion rule was then introduced to combine these features to generate a matching probability for the re-identification purpose. To account for the large variability in travel time, Sumalee and Wang (2012) have also introduced a fixed time window constraint to reduce the computational time of the vehicle matching problem. However, it is noteworthy that the aforementioned VRI systems are designed specifically for the purpose of traffic data collection (e.g. travel time). To our knowledge, very few studies were explicitly conducted to investigate the potential feasibility of utilizing VRI system for incident detection. Also, as the existing VRI system cannot guarantee an accurate matching due to the non-uniqueness of the signature, the mismatch between the upstream and downstream vehicles may potentially lead to the false alarms in the incident detection system.

CHAPTER 3 Data description

3.1 Study site

The Kanchanapisek expressway is one of the first expressways in Thailand equipped with automated traffic sensors. The six-lane expressway is of 35 kilometers long and is located in the suburban area in the southern side of Bangkok (see Figure 3.1). During normal traffic conditions, the expressway serves approximately 1,300 vehicles per hour, which is well under its capacity. There are twelve detector stations, six stations on each direction, along the Kanchanapisek expressway. Out of 35 kilometers of the expressway, only 24 kilometers are bounded by detector stations. The 24-km stretch is divided into ten sections of which automated traffic sensors are located at both upstream and downstream end. In this study, each of these sections is assigned with a section ID (see Figure 3.1) for easy reference. The average length for these 10 sections is approximately 5 kilometers, which is ten times longer than the typical section considered in previous studies. Expressway sections and detection station locations are listed in Table 3.1.

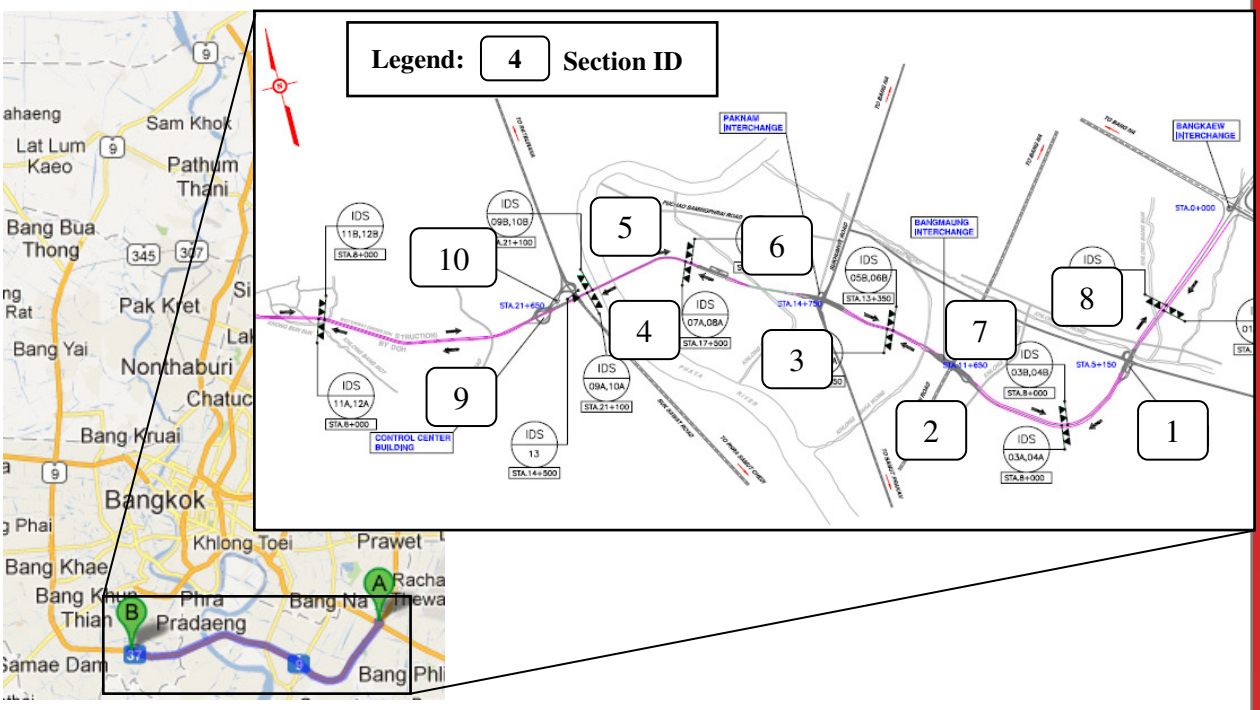

Figure 3.1 Study site. (Google Maps, 2012)

Table 3.1 Study sections and locations for detection stations (IDS stations)

Link ID	Upstream IDS Station	Downstream IDS Station	Upstream Chainage	Downstream Chainage	Direction
1	01A/02A	03A/04A	3+400	8+000	A
2	03A/04A	05A/06A	8+000	13+350	A
3	05A/06A	07A/08A	13+350	17+500	A
4	07A/08A	09A/10A	17+500	21+100	A
5	09B/10B	07B/08B	21+100	17+500	B
6	07B/08B	05B/06B	17+500	13+350	B
7	05B/06B	03B/04B	13+350	8+000	B
8	03B/04B	01B/02B	8+000	3+400	B
9	09A/10A	11A/12A	14+500	8+000 (Route 37)	A
10	11B/12B	09B/10B	8+000 (Route 37)	14+500	B

3.2 Data collection efforts

3.2.1 Traffic data

Traffic data were collected by video image processing (VIP) systems from February to July 2012. Occupancy and flow data were collected as an average over all three lanes at a single location over a one-minute aggregation level. Apart from the aggregated data, the implemented VIP system (Autoscope system) is also capable to collect per-vehicle record (PVR) data. However, due to an equipment error during the data collection period, only half of the collected traffic data was stored in a PVR format. Therefore, the research team decided to use the one-minute aggregated data, which cover a longer period of time and have more periods with incident, for model development and evaluation. The data that collected from the VIP system includes:

- Speed (km/hr)
- Vehicle length (m)
- Vehicle classification (derived from vehicle length)
- Average flow rate (veh/hr)
- Total Volume Count (veh/period)
- Arithmetic Mean Speed (km/hr)
- Vehicle Class Count (veh/period), grouped into five classes, i.e., A, B, C, D, and E
- Average Time Headway (sec)
- Average Time Occupancy (percent)
- Level of Service
- Space Mean Speed (km/hr)
- Space Occupancy (percent)
- Density (veh/km)

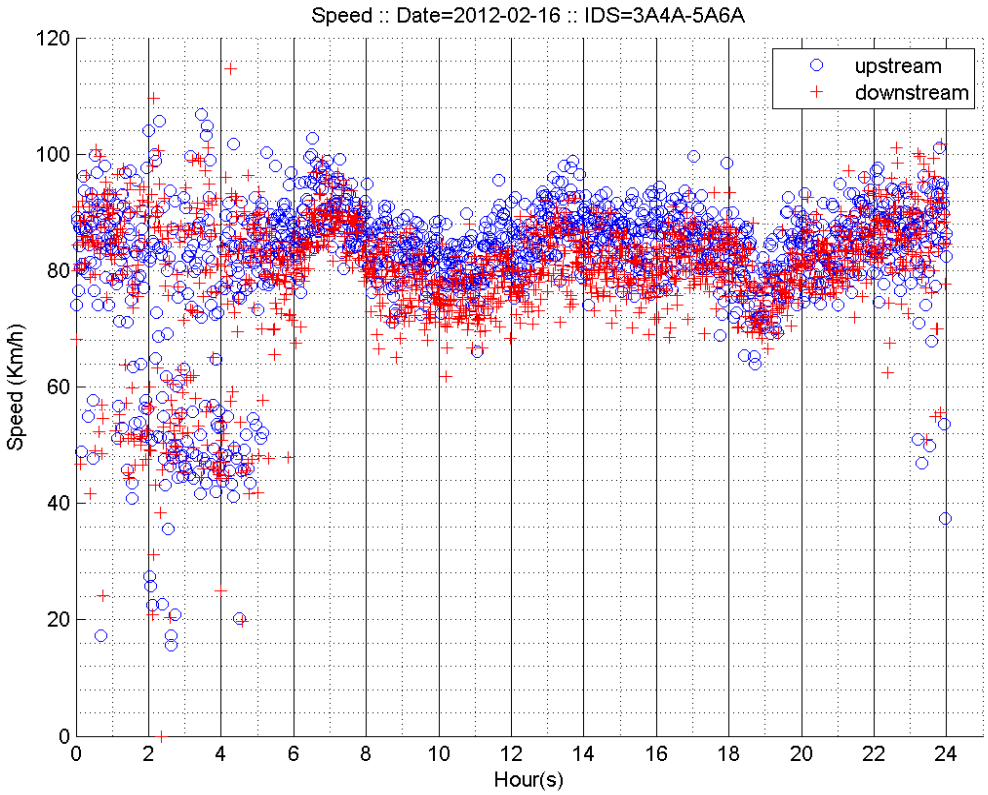

Figure 3.2 Twenty-four hour speed vs. time plot at detector station 03A/04A (upstream) and 05A/06A (downstream) on February 16, 2012

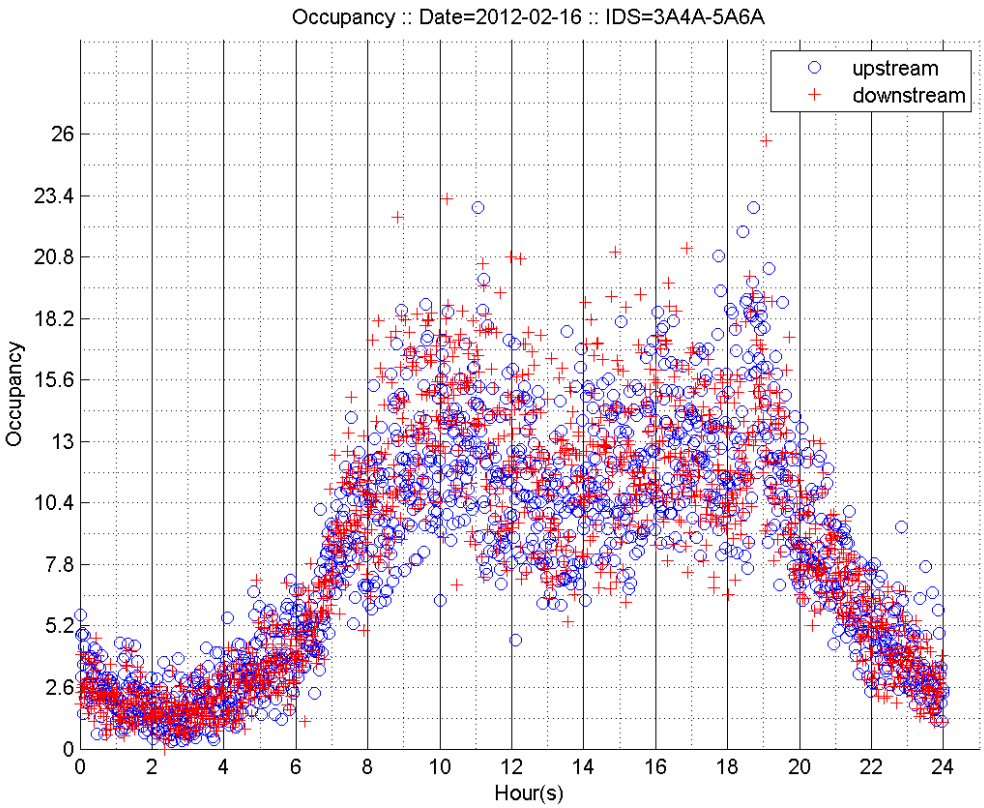

Figure 3.3 Twenty-four hour occupancy vs. time plot at detector station 03A/04A (upstream) and 05A/06A (downstream) on February 16, 2012

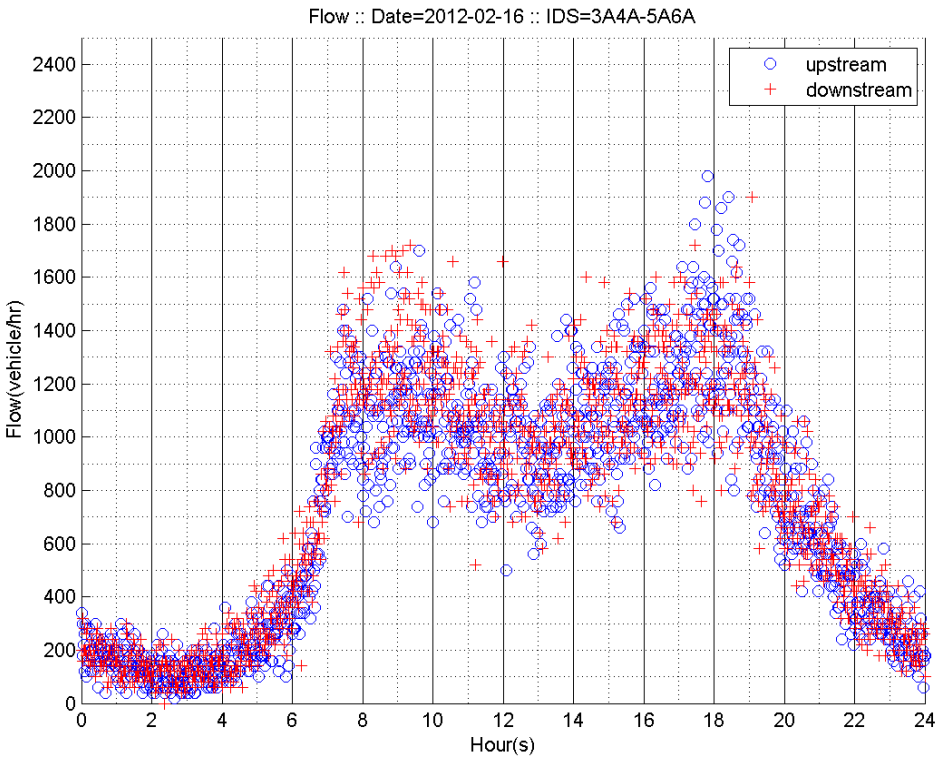

Figure 3.4 Twenty-four hour flow (veh/hr) vs. time plot at detector station 03A/04A (upstream) and 05A/06A (downstream) on February 16, 2012

Figure 3.2, 3.3 and 3.4 respectively shows the twenty-four hour plot of speed, occupancy and flow on February 16, 2012. In these figures, blue circles denote the upstream (Detector station 03A/04A) traffic characteristics while the red crosses denote the downstream (Detector station 05A/06A) data. Each of these data points (i.e. a blue circle or a red cross) is the one-minute aggregated data for the corresponding time and location. Figures 3.2 ~ 3.4 shows the typical traffic condition on section 2 (Table 3.1) on a weekday without incident. From Figure 3.2, it could be observed that the average speeds vary between 70 km/hr to 100 km/hr for the 24-hours period. The observed average speeds are relatively stable as the traffic demand is well under the capacity of the expressway and the traffics are travel at their free-flow speed. For the plot of occupancy and flow (Figure 3.3 and 3.4), there are two distinct peaks at around 9:00 and 18:00, which are respectively the morning and evening peak of traffic. Apart from the data shown in Figure 3.2 ~ 3.4, similar data are also collected for different detector stations and day of week.

3.2.2 Video data

Video data (in mpg format) are collected by the video cameras, which are installed in the IDS stations and viewed upstream, from February to July 2012. The frame rate of the recorded video is 25 FPS and the still image size is 563 × 764.

3.2.3 Incident data

Incident data during the data collection period for traffic and video data (February to July 2012) were retrieved from the incident database of the Expressway Authority of Thailand (EXAT). The attributes available from the incident database includes: time of the incident being reported, location of incident, incident type, arrival time of rescue unit, and time to clear the incident. As the proposed traffic parameter-based algorithm (Chapter 4) focuses on the capacity-reducing type of incidents, minor incidents that did not cause congestion are not included for the calibration and testing of this algorithm. During this six-month period, a total of 36 congestion-induced incidents are collected over the 10 expressway sections and the number of congestion-induced incident for each of the section is shown in Figure 3.5. From Figure 3.5, it can be seen that section 2 has the highest number of incidents (8 incidents) while its following section (section 3) has the lowest (1 incident). High number incidents on section 2 might due to the small radius of curvature right before entrance of the section. Table 3.2 shows the details of these 36 congestion-induced incidents that include: link ID for the location of incident, upstream/downstream detector station for the section of expressway with incident, date of incident, start and end time of the incident induced congestion.

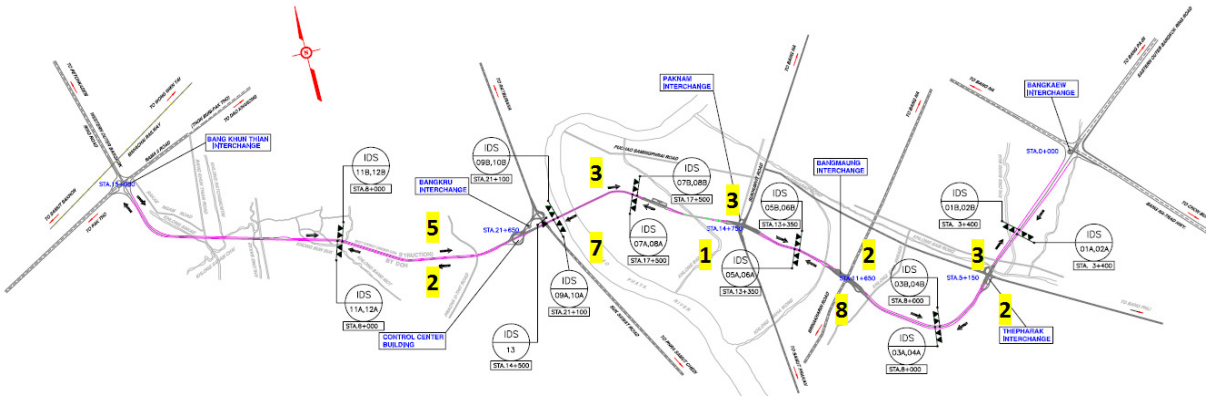

Figure 3.5 Number of congestion-induced incidents on the Kanchanapisek Expressway (From February to July 2012).

Table 3.2 Location and time of the congestion-induced incidents occurred on the Kanchanapisek Expressway (From February to July 2012)

Link ID	Upstream/Downstream	Date	Start Time	End Time
1	1A2A/3A4A	28/4/2012	12:10	12:30
1	1A2A/3A4A	23/6/2012	7:15	7:30
2	3A4A/5A6A	26/3/2012	14:10	19:20
2	3A4A/5A6A	30/3/2012	18:30	19:30
2	3A4A/5A6A	31/3/2012	16:00	21:00
2	3A4A/5A6A	27/4/2012	18:00	20:00
2	3A4A/5A6A	30/4/2012	18:00	20:00
2	3A4A/5A6A	2/5/2012	18:30	19:20
2	3A4A/5A6A	11/7/2012	12:40	13:10
2	3A4A/5A6A	13/7/2012	18:15	19:00
3	5A6A/7A8A	31/3/2012	15:30	16:00
4	7A8A/9A10A	21/2/2012	12:20	14:50
4	7A8A/9A10A	17/3/2012	11:15	11:45
4	7A8A/9A10A	27/4/2012	12:45	12:50
4	7A8A/9A10A	15/6/2012	16:30	18:00
4	7A8A/9A10A	18/6/2012	16:45	17:15
4	7A8A/9A10A	25/6/2012	17:10	17:50
4	7A8A/9A10A	13/7/2012	15:00	15:45
5	9B10B/7B8B	15/3/2012	11:00	13:30
5	9B10B/7B8B	30/4/2012	14:50	15:30
5	9B10B/7B8B	11/7/2012	9:40	10:00
6	7B8B/5B6B	19/3/2012	13:55	15:00
6	7B8B/5B6B	3/5/2012	16:15	18:10
6	7B8B/5B6B	19/6/2012	11:00	11:30
7	5B4B/3B4B	27/3/2012	11:45	12:50
7	5B4B/3B4B	18/6/2012	12:10	13:30
8	3B4B/1B2B	7/3/2012	7:00	10:50
8	3B4B/1B2B	22/6/2012	11:58	12:36
8	3B4B/1B2B	26/6/2012	11:57	12:22
9	9A10A/11A12A	15/3/2012	11:40	12:00
9	9A10A/11A12A	26/3/2012	13:20	13:40
10	11B12B/9B10B	18/3/2012	13:20	13:30
10	11B12B/9B10B	15/6/2012	11:45	12:30
10	11B12B/9B10B	21/6/2012	9:00	10:00
10	11B12B/9B10B	1/7/2012	15:30	16:00
10	11B12B/9B10B	12/7/2012	15:45	19:00

Apart from the congestion-induced incidents used for the development of TP-based incident detection algorithm, this study also extracts the non-congestion-induced incidents from the EXAT incident database for the validation of VRI-based incident detection algorithm (Chapter 5). Non-congestion-induced incident is the kind of incident that has no observable impact on the upstream/downstream traffic conditions (i.e. speed, occupancy, etc). Table 3.3 shows the details of the 2 non-congestion-induced incidents used in the validation. For Table 3.3, it could be observed

that this kind of incidents mainly happen during off-peak hours (i.e. 16:30) or weekend (i.e. Sunday, 17-06-2012).

Table 3.3 Location and report time of the non-congestion-induced incidents occurred on the Kanchanapisek Expressway (From February to July 2012)

Link ID	Upstream/Downstream	Date	Report Time
4	7A8A/9A10A	13/6/2012	16:03
4	7A8A/9A10A	17/6/2012	10:31

CHAPTER 4 Development of traffic parameter-based (TP-based) algorithm for incident detection

4.1 Introduction

In this chapter, the traffic parameter-based (TP-based) algorithm is developed for incident detection of an expressway system in Bangkok. The proposed algorithm will mainly be used for detecting the congestion-induced incidents of which the occurrence of incidents will have substantial impacts to the traffic conditions (e.g. flow, occupancy, etc) detected by traffic sensors. In this chapter, three different incident detection algorithms: California algorithm, McMaster algorithm and Rule-based McMaster algorithm will be proposed for incident detection on Kanchanapisek expressway in Bangkok (Section 4.2, 4.3 and 4.4). A performance measure for these incident detection algorithms are proposed in Section 4.5 for evaluating and calibrating the proposed algorithms.

4.2 California algorithm

In California algorithm, the differences between upstream and downstream occupancies are monitored over time for incident detection. When there is an incident occurred on a road stretch, the upstream occupancy will increase significantly while the downstream occupancy will decrease in a short time. Figure 4.1 shows the occupancy vs. time (a) and speed vs. time (b) plot of section 2 of the Kanchanapisek Expressway on March 26, 2012. In this figure, blue circles denote the data collected from the upstream detector station while red crosses represent data from the downstream. In Figure 4.1a, it could be observed that from 14:00 to 19:30, the occupancies of the upstream detector (blue circles) suddenly increase from 10% to over 30% and with a much larger fluctuation. For the downstream occupancies (red crosses) at this period, they are generally the same, or slightly dropped, as compared to the other periods (before 14:00 or after 19:30). Such sudden change of occupancy in upstream/downstream detector station could be explained by the incident happens on this section of expressway at around 14:10 (see Table 3.2). After the incident happens, the capacity of the expressway drops and create a bottleneck at the location of incident. As a result, vehicles move slower before the bottleneck and cause a higher occupancy at the upstream detector. The incident happens in this section of expressway will also affect the speeds collected in the upstream and downstream ends (Figure 4.1b). Unlike occupancy, the speeds collected by the upstream detector drop tremendously after the incident happens (see blue circles after 14:00 in Figure 4.1b).

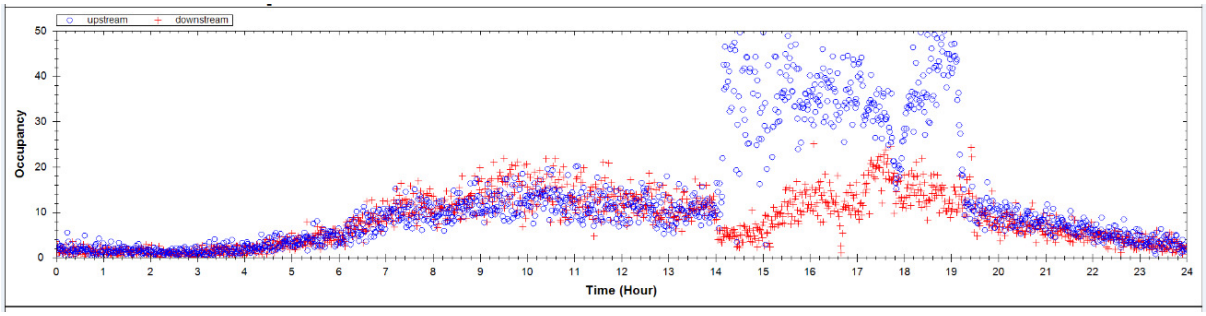

(a)

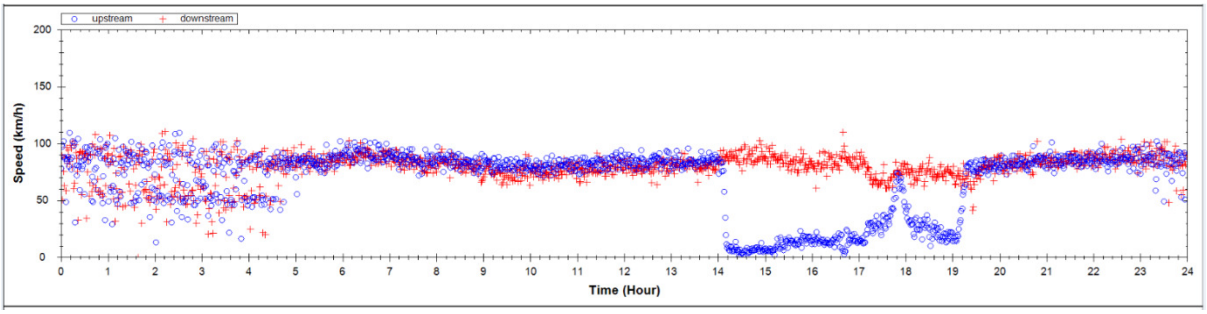

(b)

Figure 4.1 Traffic conditions during incident and non-incident traffic.

California algorithm has made use of the aforementioned observable changes in occupancies for detecting an incident. The California algorithm (Payne and Tignor, 1978) was among the first incident detection algorithms developed in 1970's and has been adopted by several traffic management centers (Guin, 2004, Mahmassani et al., 1995, Martin et al., 2001). In a traditional California algorithm, three types of spatial/temporal occupancy differences are checked (Weil et al., 1998):

- Spatial difference between upstream and downstream occupancies, $OCCDF(i,t)$, and is defined as:

$$OCCDF(i,t) = OCC(i,t) - OCC(i+1,t)$$

- Spatial difference between upstream and downstream occupancies relative to the upstream occupancy, $OCCRDF(i,t)$, and is defined as:

$$OCCRDF(i,t) = \frac{OCCDF(i,t)}{OCC(i,t)}$$

- Temporal difference between downstream occupancies at time *t* and (*t*-2) relative to the downstream occupancy at time (*t*-2), $DOCCTD(i,t)$, and is defined as:

$$DOCCTD(i,t) = \frac{OCC(i+1,t-2) - OCC(i+1,t)}{OCC(i+1,t-2)}$$

These occupancy differences will be compared with the pre-determined thresholds (i.e. T_1, T_2, and T_3), which will be determined by optimizing an objective function based on the empirically collected incident and traffic data, for identifying an incident.

There are numerous comparative algorithms developed based on this principle. In this study, one of the California Algorithms described in the comprehensive review in Parkany and Xie (2005) is selected due to its simplicity. The flow chart of the California algorithm used in this study is shown in Figure 4.2. In this figure, the parameter i denotes the time slot index while U_i^{occ} and D_i^{occ} respectively denotes the upstream and downstream occupancy at time slot i. At the first step, the absolute difference in occupancies between the upstream and downstream stations, $\left(U_i^{occ} - D_i^{occ}\right)$, is compared with the threshold T_1. If this absolute difference is less that the threshold, potential incident for this time slot (Pi) will be set as false and check for the next time slot. Otherwise, the comparisons of the other occupancy differences are performed. Next, the relative difference in occupancy between the upstream and downstream stations with respect to the upstream value, $\left(U_i^{occ} - D_i^{occ}\right)/U_i^{occ}$, is compared with the threshold T_2. Similarly, if the relative difference is less than the threshold, potential incident for this time slot (Pi) will be set as false and check for the next time slot. Finally, the relative difference in occupancy between the upstream and downstream stations with respect to the downstream value, $\left(U_i^{occ} - D_i^{occ}\right)/D_i^{occ}$, is compared with the threshold T_3. If this relative difference is less the threshold (T_3), potential incident for this time slot will be set as false. Otherwise, the incident alarm will be issued (i.e. $Pi = True$) for this time slot and go to check for the next time slot. In this algorithm, the thresholds (T_1, T_2, and T_3) will be determined by maximizing the composite index (CI) defined in Section 4.5.

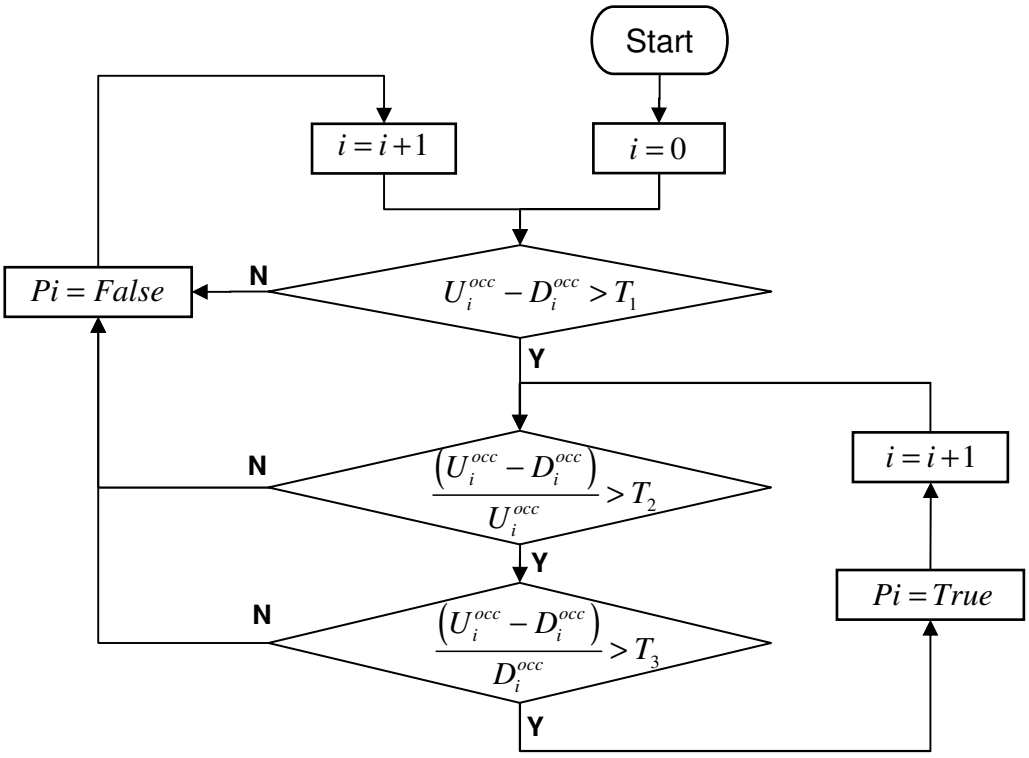

Figure 4.2 Flow chart of the California Algorithm used in this study.

4.3 McMaster algorithm

The McMaster algorithm (Forbes, 1992; Persaud and Hall, 1989; Hall et al., 1993) determines anomalies in traffic flow using the Catastrophe theory. Traffic state of upstream and downstream detector stations is determined from the flow-occupancy plot. Figure 4.3 shows the typical flow-occupancy template used in the McMaster algorithm for determining the traffic states of a particular location. In this figure, it could be seen the traffic states are determined based on the following traffic characteristics of the study location: maximum uncongested occupancy ($OCMAX$), minimum discharge volume ($Vcrit$), and minimum uncongested volume threshold ($g(OCC)$). Based on these characteristics, the definition and characteristics of each traffic states is defined as follows:

- State 1 is the state that occupancy is less than $OCMAX$ while the volume is greater than $g(OCC)$ function. This state usually occurs during the uncongested condition.
- State 2 is the state that occupancy is less than $OCMAX$ and the volume is also less than $g(OCC)$ function. This state usually occurs during the congested condition.
- State 3 is the state that occupancy is greater than $OCMAX$ while the volume is less than $Vcrit$ threshold. This state potentially indicates an incident occurrence.

- State 4 is the state that occupancy is greater than $OCMAX$ and the volume is greater than $Vcrit$ threshold. This state is usually the result of the bottleneck flow.

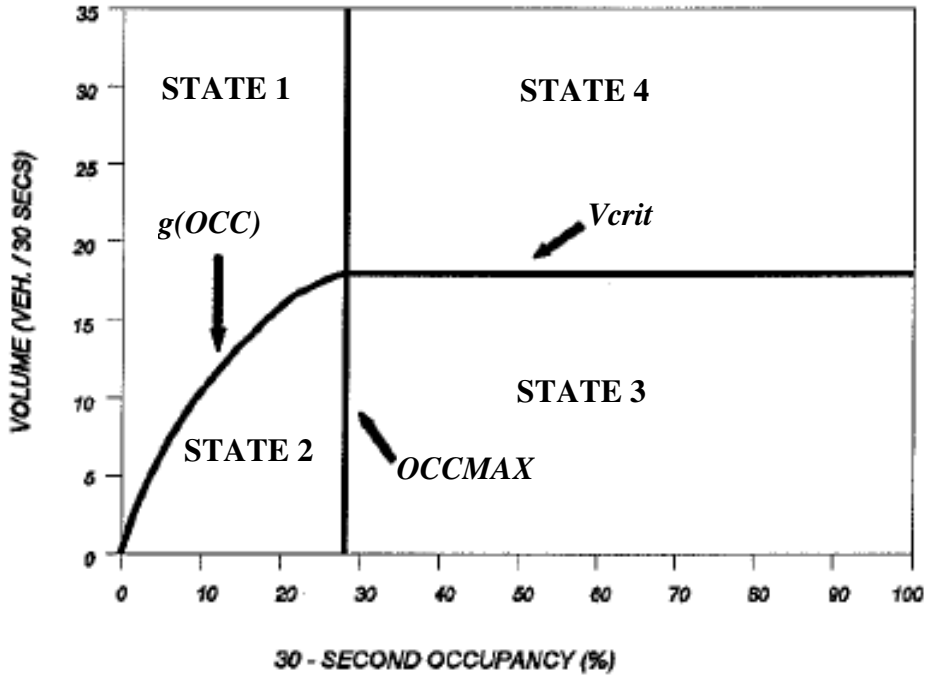

Figure 4.3 Flow-occupancy template for McMaster's algorithm (Balke, 1993).

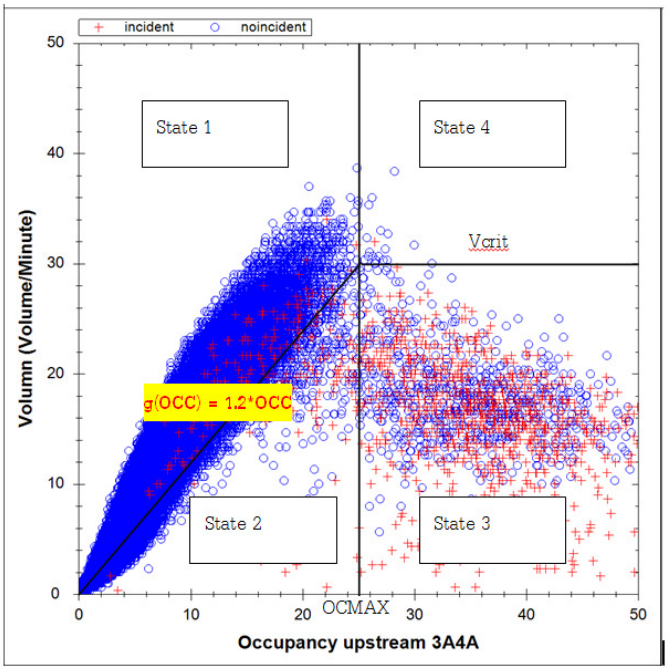

Figure 4.4 Flow-occupancy diagram and the four McMaster's traffic states at detector station 3A4A.

Figure 4.4 shows the 1-minute aggregated flow-occupancy plot for detector station 3A4A. In this figure, data collected under incident-free environment is denoted by blue circles while red crosses represent data collected during an incident. The three quantities ($OCMAX$, $Vcrit$ and $g(OCC)$) used for defining the McMaster's traffic states is determined by maximizing the composite index (CI)

defined in Section 4.5. Based on the traffic states determined at the upstream and downstream detector stations, a decision matrix is adopted to determine the incident state of the road section bounded by these two stations (Table 4.1). For the upstream traffic state equal to 2 or 3, the McMaster algorithm will mark the road section to have incident if the downstream traffic state is equal to 1 or 2. For the upstream traffic state equal to 1 (4), no matter what is the traffic state for the downstream location, the road section will be concluded to have an uncongested (bottleneck) flow of traffic. On the other hand, for the downstream traffic state equal to 3 (with traffic state of upstream equals to 2 or 3), the analysis for this section is not conclusive and should check the traffic state for the i+2 station. Finally, for the downstream traffic state equal to 4 (with traffic state of upstream equals to 2 or 3), the section are concluded to have recurrent congestion. In this study, the flow chart in Figure 4.5 is adopted for determining the traffic states in the McMaster algorithm. For each time slot (1 minute in this study), the aggregated occupancy and volume of each detector stations are compared with the calibrated parameters of that detector station ($OCMAX$, $Vcrit$ and $g(OCC)$) for determining the corresponding traffic state.

Table 4.1 Decision matrix for incident detection in McMaster algorithm

Downstream (Station i+1) Traffic State	Upstream (Station i) Traffic State			
	1	2	3	4
1	Uncongested	INCIDENT	INCIDENT	Bottleneck flow
2	Uncongested	INCIDENT	INCIDENT	Bottleneck flow
3	Uncongested	Check downstream station i+2	Check downstream station i+2	Bottleneck flow
4	Uncongested	Recurrent Congestion	Recurrent Congestion	Bottleneck flow

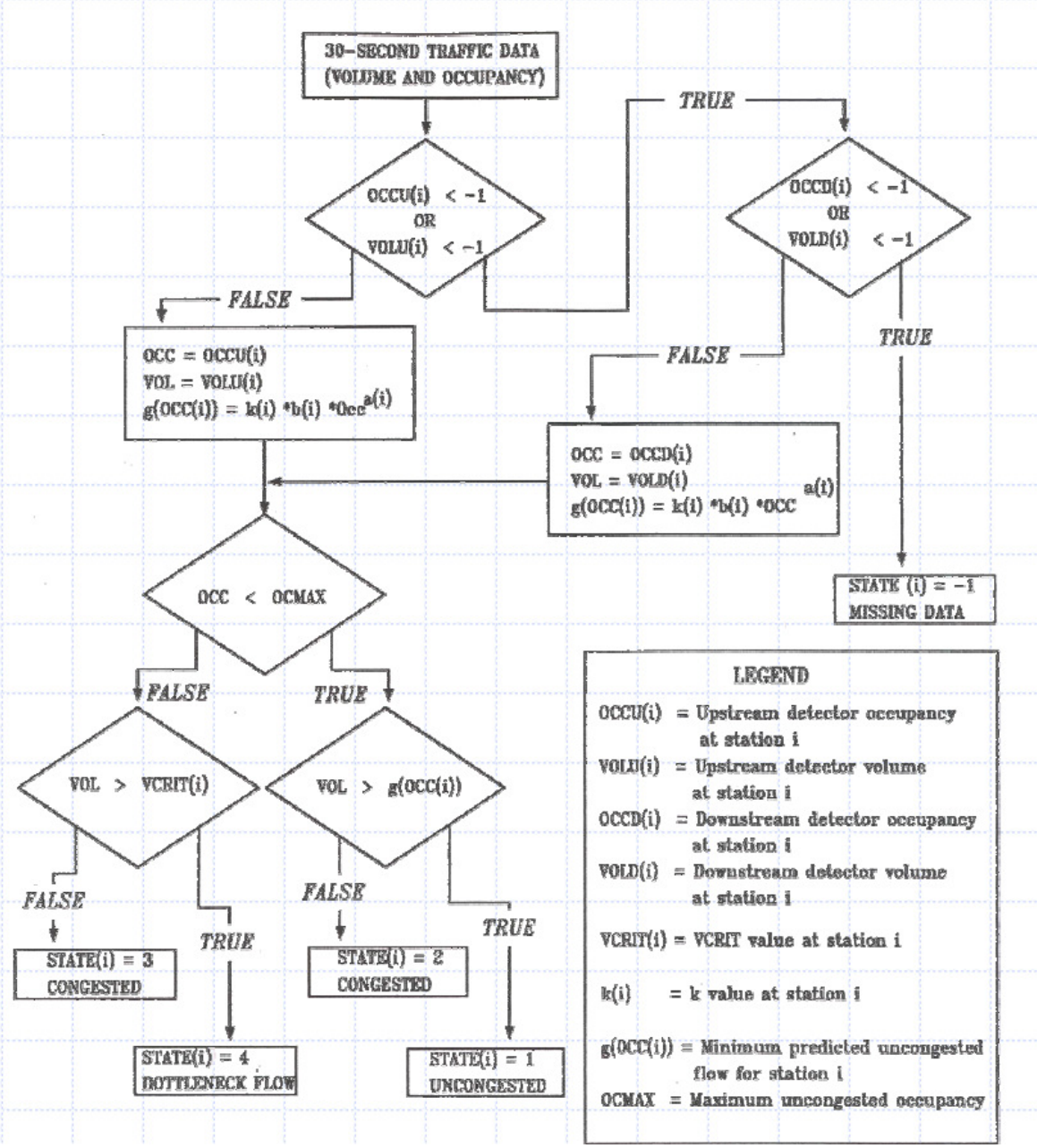

Figure 4.5 McMaster algorithm flow chart.

4.4 Rule-based McMaster algorithm

To improve the performance of McMaster algorithm, the research team took a closer look at the flow versus occupancy plots of all expressway sections. Figure 4.6 illustrates the flow-occupancy plots at the upstream (3A4A) and downstream (5A6A) detector stations for section 2 of the studied expressway. In this figure, data collected under incident-free environment is denoted by blue circles while red crosses represent data collected with incident occurred in section 2. The traditional McMaster algorithm gives a binary result of either “one” (i.e. incident occurrence) or “zero” (i.e., non-incident occurrence). This implies that all four combinations of upstream/downstream traffic states (red boxes in Table 4.1) have an equal weight. However, from Figure 4.6, it could be seen

that such assumption of equal weight is not realistic. During incidents (red crosses in Figure 4.6), majority of upstream traffic are in state 3, which is the congested traffic condition (lower right portion of Figure 4.6a), while the majority of downstream traffic are in state 1, which is the uncongested condition (upper left portion of Figure 4.6b). As compared to the other combinations, this combination of traffic states (i.e. congested at the upstream location and uncongested at the downstream location) is the most obvious form as incident occurs (Weil et al., 1998). Therefore, it would be more reasonable to assign a different weight (or confidence level) to different combinations of traffic states in identifying an incident.

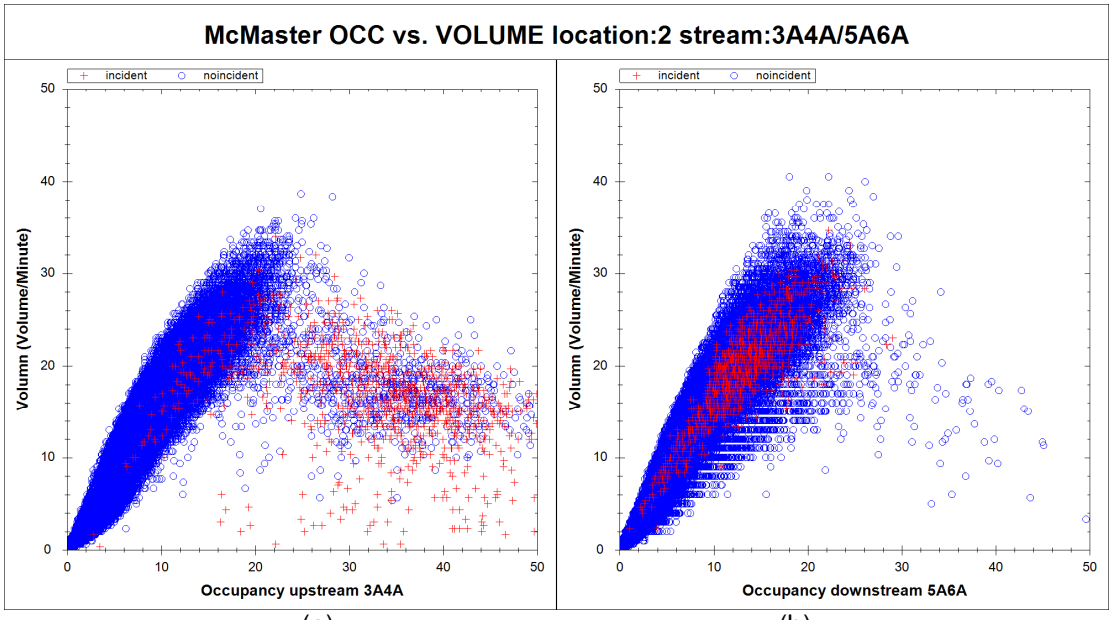

(a) (b)

Figure 4.6 Flow-occupancy plot for the upstream (a) and downstream (b) detector station of section 2.

Based on the observations discussed in the previous paragraph, the Rule-Based Confident Index (RCI) for the McMaster algorithm is introduced for each of the four traffic state combinations (red boxes in Table 4.1). The RCI is between 0 and 1 and can be estimated in the following two steps

Step 1: For each traffic state combination, the proportion of time slots with the correctly-detected incident under that traffic state combination is calculated. For example, if there are 450 out of 1000 time slots with correctly-detected incident occur under the situation that upstream is at state 3 and downstream is at state 1, then the proportion for this combination will be 0.45.

Step 2: The maximum value of the four proportions determined in the first step is then used to standardize these proportions to obtain the corresponding RCIs. One of the RCIs will has the maximum value of 1 as it is the traffic state combination with the largest proportion of time slots of correctly-detected incident.

It is noteworthy that: i) RCI will be estimated base on all available correctly-detected incidents from different locations (i.e. location independent) and, ii) a larger value of RCI indicates a higher chance of having incident under that traffic state combination.

In the McMaster algorithm discussed in Section 4.3, a road section will be identified to have incident if the combination of upstream and downstream traffic states is one of the four combinations (red boxes) shown in Table 4.1. The proposed Rule-based McMaster algorithm will follow the same procedure as in the McMaster algorithm (Section 4.3) but make use of the developed RCI for the final decision of incident detection. In the proposed Rule-based McMaster algorithm, the RCI of road sections will be compared with an adaptive threshold, T_a, for determining the incident status of that section. The incident status can be determined by applying the following rule:

$$\text{IF } (RCI_{i,t} \geq T_a) \text{ THEN (Incident Status = 1) ELSE (Incident Status = 0)} \quad (4.1)$$

where $RCI_{i,t}$ denotes the RCI of road section *i* at time *t*, which is based on the upstream and downstream traffic states at that time. Incident status equals to 1 indicates an incident occur while 0 indicates there is no incident. The adaptive threshold T_a is specifically defined for each of the road section between detector stations and will be determined by maximizing the composite index (CI) defined in Section 4.5.

4.5 Performance measures

In the literature, the performances of incident detection algorithms are commonly measured by the following three indices (Mahmassani et al., 1995):

- **Detection rate (DR)** – Detection rate is defined as the number of detected incidents divided by the total number of actual incidents. In this study, only correctly detected incidents are counted as detected incidents. The falsely detected incidents were not included since it would mislead the actual algorithm performance. The detection rate will range from zero to one and a higher value indicates a more effective algorithm. For analyzing the TP-based algorithms, the detection rate is defined by the following equation:

$$DR = \frac{Number\ \ of\ \ detected\ \ incidents}{Total\ \ number\ \ of\ \ actual\ \ incidents}$$

- **False alarm rate (FAR)** – False alarm rate is defined as the number of time slots with incidents being falsely declared divided by the total number of time slots (or the total

number of algorithm applications). The false alarm rate will range from zero to one and a smaller value indicates a more effective algorithm. For analyzing the TP-based algorithms, the false alarm rate is defined by the following equation:

$$FAR = \frac{Number\ \ of\ \ time\ \ slots\ \ with\ \ incidents\ \ falsely\ \ declared}{Total\ \ number\ \ of\ \ time\ \ slots}$$

- **Mean time to detect (TTD)** – Mean time to detect is defined as the average difference between the beginning times of the detected incident and actual incident. The TTD will range from zero to infinity and a smaller TTD indicates a more efficient algorithm. For analyzing the TP-based algorithms, the TTD is defined by the following equation:

$$TTD = Average\left(T_{Detected} - T_{Actual}\right)$$

To determine the required parameters (e.g. T_1, T_2, T_3 for California algorithm; $OCMAX$, $Vcrit$ for McMaster algorithm; T_a for Rule-based McMaster algorithm) in each algorithm for optimizing their overall performance, a single objective function has to be defined. In this study, the Composite Index (CI) was proposed by combining the above three performance indices (DR, FAR and TTD) and is defined as follow:

$$CI = \frac{DR\left(1 - FAR\right)}{e^{\frac{TTD}{Max(TTD)}}} \tag{4.2}$$

As mentioned previously, the algorithms discussed in Section 4.2 ~ 4.4 will be calibrated by maximizing the CI defined in Equation 4.2. By maximizing the CI, the detection rate will be maximized, while the false alarm rate and mean time to detect will be minimized. CI will range from zero to one and a higher value indicates a better overall algorithm performance.

4.6 Summary

In this section, three different traffic parameter-based (TP-based) incident detection algorithms are introduced for the implementation in the Kanchanapisek Expressway. California algorithm detects an incident by considering the temporal and/or spatial changes of occupancies. McMaster algorithm detects an incident by considering the traffic states, which is defined by the occupancies and flows, at the upstream and downstream ends of the section. Rule-based McMaster algorithm has extended the McMaster algorithm by introducing a Rule-Based Confident Index in incident detection. For calibrating the incident detection algorithms introduced in this section, Composite

Index, which is the combination of the three commonly used indices (detection rate, false alarm rate and mean time to detect), is proposed.

CHAPTER 5 Development of vehicle reidentification-based (VRI-based) algorithm for incident detection

5.1 Introduction

In the chapter, the vehicle reidentification-based (VRI-based) algorithm is developed for incident detection in a closed expressway system. The proposed algorithm will mainly be used in the non-congested, or free-flow, traffic conditions such that the occurrence of incidents will not induce any congestions/delays that could be detected by the traffic sensors (e.g. increase in occupancies). In this chapter, the required data structure will be described in Section 5.2, while the framework for the proposed VRI-based incident detection algorithm will be introduced in Section 5.3. The two main components of the proposed framework, flexible time window estimation and vision-based vehicle re-identification, will introduce in Section 5.4 and 5.5, respectively.

5.2 Data structure

In this study, video image processing systems (VIPs) are adopted for extracting the required information of the proposed VRI-based incident detection algorithm. In general, the VIPs involve two major steps: detection and feature extraction. The first step is to digitize and store the raw video record for the detection subsystem to detect and capture the moving vehicles. For each of the captured vehicles, still image regarding that individual vehicle is stored for further usage. In the second step, various image processing techniques are performed on the vehicle images to obtain the intrinsic feature data (e.g. color, length and type). In the following, a brief review on the VIPs and the associated image processing techniques is presented.

5.2.1 Video Image Processing Systems (VIPs)

Vehicle Detection

The success of vehicle detection largely depends on the degree that the moving object (vehicle) can be distinguished from its surroundings (background). In light of this, background estimation technology is employed in the detection subsystem. By calculating the media of a sequence of video frames, the background of the video image is obtained. Then image segmentation technique is performed to identify the foreground object (vehicle). The still image including the detected vehicle is then clipped and stored for further feature extraction. Along with the detected vehicle, the associated arrival time, t, and the spot speed, v, are also collected. It is obvious that the vehicle length, L, is simply the height of the vehicle image.

Vehicle Color Recognition

Color is one of the most essential features for characterizing a vehicle. To reduce the negative effect of illumination changes, this study has adopted the HSV (hue-saturation-value) color space to represent the vehicle image. Vehicle color recognition adopted in this study is conducted in two separate steps. First, the general RGB color images are converted into HSV color model-based images. Hue and Saturation values are then exploited for color detection, while V (value) information is separated out from the color space. Second, a two-dimensional color histogram C is formed to represent the distribution (frequency) of colors across a vehicle image. To be more specific, the hue and saturation channels are divided into 36 and 10 bins, respectively. Thus, a color feature vector, C, with 360 elements is obtained.

Vehicle Type Recognition

Apart from the vehicle color, vehicle type provides the other important information to describe a vehicle. In this study, the template matching method is utilized to recognize vehicle type. This method uses $L2$ distance metric to measure the similarity between vehicle image and template images. In this study, vehicles are classified into 6 categories and, for each categories, the corresponding template image (T) is built. Finally, the normalized similarity value between the vehicle image (I) and the kth template image (T) is given by:

$$S(k) = \frac{\sum_{m=1}^{\mathcal{M}} \sum_{n=1}^{\mathcal{N}} |I(m,n) - T(m,n)|^2}{\mathcal{G}\mathcal{M}\mathcal{N}} \tag{5.1}$$

where $\mathcal{G}$ denotes the maximum gray level (255); $\mathcal{M}$ and $\mathcal{N}$ are the dimensions of the vehicle image. Thus, the vehicle type/shape feature, S, is a vector that consists of the similarity score for each template. Detailed implementation of the VIP systems to traffic data extraction can be found in Sumalee and Wang (2012). A formal description of the dataset obtained from the video record is presented in the following subsection.

5.2.2 Dataset description

VIPs provide a large number of necessary traffic data to develop and validate the proposed VRI-based incident detection algorithm. Let $U = \{1, 2, \cdots, N\}$ denotes the set of N vehicles detected at upstream station during the time interval, while $D = \{1, 2, \cdots, M\}$ is the set of downstream vehicles. In addition, t_i^U and v_i^U are the associated arrival time and spot speed of the ith upstream vehicle, respectively. Accordingly, t_j^D and v_j^D are the corresponding arrival time and spot speed of the jth

downstream vehicle. As discussed earlier, for each detected individual vehicle, the intrinsic feature data (e.g. color, size, length) are also obtained. Let $X_i^U = \{C_i^U, S_i^U, L_i^U\}$ denotes the signature of the ith upstream vehicle, where C_i^U and S_i^U are respectively the normalized color feature vector and type (shape) feature vector. L_i^U denotes the normalized length of vehicle i. Similarly, $X_j^D = \{C_j^D, S_j^D, L_j^D\}$ is the signature of the jth downstream vehicle. To sum up, dataset from the VIPs during a time interval consists of the upstream vehicle dataset $\left\{\left(t_i^U, v_i^U, X_i^U\right), i=1,2,\cdots,N\right\}$ and the downstream vehicle dataset $\left\{\left(t_j^D, v_j^D, X_j^D\right), j=1,2\cdots M\right\}$. In order to quantify the difference between each pair of upstream and downstream vehicle signatures, several distance measures are then incorporated. Specifically, for a pair of signatures (X_i^U, X_j^D), the Bhattacharyya distance (Bhattacharyya, 1943) is utilized to calculate the degree of similarity between color features:

$$d_{color}(i,j) = \left[1 - \sum_{k=1}^{360} \sqrt{C_i^U(k).C_j^D(k)}\right]^{1/2} \tag{5.2}$$

where k denoted the kth component of the color feature vector. The $L1$ distance measure is introduced to represent the difference between the type feature vectors:

$$d_{type}(i,j) = \sum_{k=1}^{q} |S_i^U(k) - S_j^D(k)| \tag{5.3}$$

where q is the number of vehicle type template and is taken as 6 in this study. The length difference is given by:

$$d_{length}(i,j) = | L_i^U - L_j^D | \tag{5.4}$$

For the development/calibration of the VRI-based incident detection algorithm in this chapter, a 3.6-kilometer-long section of the closed three-lane expressway in Bangkok, Thailand (section 4 and 5 in Figure 3.1) is taken as the test site. At the upstream and downstream end of these sections, two hours of video record (10 AM to 12 Noon, on March 15, 2011) was used for model calibration. Based on the videos collected at the test site, 3,628 vehicles are detected at both stations (10B and 8B) during the two-hour video record. For the purpose of the algorithm development and evaluation, these 3628 pairs of vehicles are manually matched (i.e. re-identified) by the human operators viewing the video record frame by frame. In other words, the ground-truth matching result of the 3,628 pairs of vehicles are obtained in advance. The mean travel time is 170.9 seconds. The first 800 pairs of vehicle data are used for the model training and calibration (which are discussed

in the following sections), while the rest of vehicle dataset are used for the simulation test of the proposed VRI-based incident detection algorithm (Section 6.2).

5.3 Framework for VRI-based incident detection system

The basic idea of the proposed VRI-based incident detection is to track the individual vehicle so as to identify the missing vehicle due to an incident. Similar approach could also be found in vehicle count approach (Fambro and Ritch, 1980), which is well-known for its computational and theoretical simplicity. Thus, it is necessary to revisit this method in detail before the development of the development of the VRI-based algorithm.

5.3.1 Vehicle count approach

The basic operation of the vehicle count approach is illustrated in Figure 5.1. When a vehicle U_i arrives at the upstream station at time t_i^U , the expected arrival time window $[Lb_i, Ub_i]$ of this vehicle at downstream station is estimated. Lb_i and Ub_i are respectively the lower and upper bound of the arrival time window. If another vehicle U_j is detected at upstream station, the corresponding arrival time window $[Lb_j, Ub_j]$ can also be obtained. Unsurprisingly, there may be overlap between these two time windows, and both of these two vehicles are likely to arrive at downstream during time interval $[Lb_j, Ub_i]$. The incident would then be detected by comparing the collected vehicle count data to the expected number of vehicles in a time interval. In the case that vehicle U_i is missing, if vehicle U_j arrives at downstream during time interval $[Lb_j, Ub_i]$, then the incident alarm will not be triggered until time Ub_j, which is clearly later than the upper bound of the arrival time widow of vehicle U_i (i.e. Ub_i). Because of the overlapping between the time windows, the vehicle count approach, which is solely based on comparing the vehicle counts data, cannot promptly detect the incident (i.e. delay in incident detection). In general, the incident detection time would significantly increase with respect to the increase in size of vehicle platoon at the upstream detector, which increases the number of overlapping in arrival time intervals at the downstream detector.

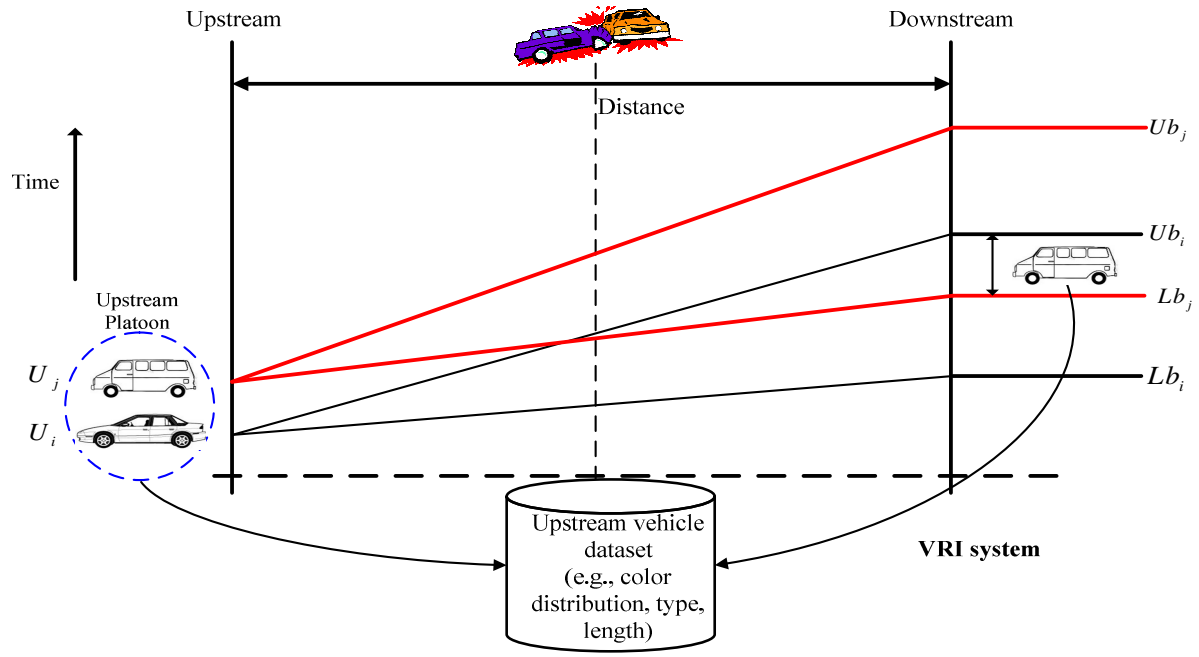

Figure 5.1 Illustrative example of vehicle count approach.

To reduce the detection time, this research proposes a new incident detection algorithm by incorporating the vision-based VRI system. As shown in Figure 5.1, vehicle U_i and U_j are detected and their detailed feature data (e.g. color, type and length) are also extracted. Once a vehicle is detected at downstream site, the proposed VRI system is performed to find a matched upstream vehicle based on the vehicle feature data. In the case that vehicle U_i is missing, if the downstream vehicle could be matched to vehicle U_j based on the vehicle feature, an incident alarm would be triggered at time Ub_i, as vehicle U_i is not re-identified during time window $[Lb_i, Ub_i]$.

5.3.2 Incident detection algorithm based on VRI system

The detailed implementation of the VRI-based incident detection system is summarized in the following flowchart (Figure 5.2). First, the system will initialize the timestamp, t, and check whether a vehicle is detected at the upstream and/or downstream station. If a vehicle is detected at upstream detector, the expected arrival time window of this vehicle at downstream station will be estimated based on the historical data (Section 5.4). The record of the detected vehicle at upstream will be stored in the database as unmatched upstream vehicle. On the other hand, if a vehicle is captured at the downstream station, the system will perform the Vision-based VRI subsystem (Section 5.5) to check whether this detected vehicle match with any of the unmatched upstream vehicle. The time window constraint is utilized to identify the potential matches for this detected vehicle at downstream station. Once the match is found, the matched vehicle data will be removed from the list of the unmatched upstream vehicles.

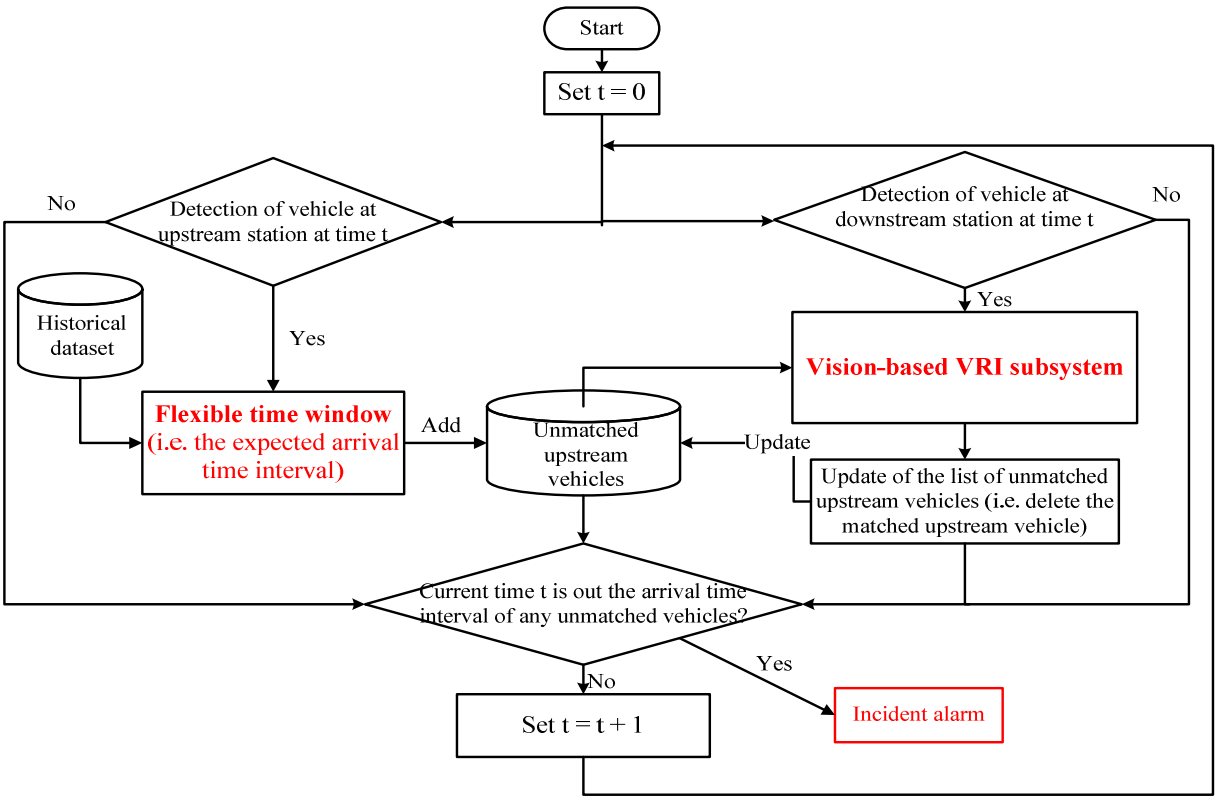

Figure 5.2 Overall framework for VRI-based incident detection system.

After the previous two steps for handling the detected vehicles at upstream and downstream station, the system will proceed to determine whether there is an incident occurs on the monitored segment. For incident detection, the system will screen through the list of unmatched vehicles. If the current time (t) is out of the expected arrival time window (i.e. greater than the upper bound of the arrival time interval) of the unmatched vehicle, an incident alarm will be issued. If not, t will be set to t+1 and the system will move forward to the next time step. It could be easily observed that the performance of the incident detection system is heavily dependent on two critical components: flexible time window constraint (Section 5.4) and vision-based VRI system (Section 5.5).

For the aforementioned framework, the following three comments should be taken into account. First, the detection error is not considered in this study. In other words, it is assumed that all the vehicles cross the video cameras will be detected. This is achievable under non-congested condition, as there is no occlusion between the vehicles. Thus, the VIPs perform generally well and are able to detect most of the individual vehicles. Second, under non-congested condition, the travelling behavior of the individual vehicle is more predictable. This phenomenon enables the estimation of the flexible arrival time window for each individual vehicle based on the current spot speed and the historical data. It is expected that the accurate estimation of the arrival time window could potentially lead to an improved matching accuracy of the VRI method, and hence reduce the incident detection time. Third, it should be noted that the proposed vehicle re-identification cannot guarantee an accurate matching because of the non-uniqueness of the vehicle signature. Instead,

the proposed VRI scheme in this study can only provide the matching probability between the downstream and upstream vehicles. Therefore, some of the mismatches resulted from the matching probability could potentially lead to false alarms. To handle this, a ratio method (Section 5.5) is introduced to screen out those mismatches for reducing the false alarms.

5.4 Flexible time window estimation

Under non-congested condition, each individual vehicle would maintain in a relatively stable speed (i.e. small travel time variability). In this case, the arrival time of the vehicle at downstream station could be estimated based on the spot speed and historical data. Let U_i represents an upstream vehicle detected at time t_i^U, and the associated upstream spot speed is denoted as v_i^U. The expected arrival time Arr of vehicle U_i is given by:

$$Arr = t_i^U + \frac{l}{0.5\left(v_i^U + v_i^D\right)} \tag{5.5}$$

where l is the distance between the upstream and downstream detector; v_i^D is the estimated vehicle speed at downstream detector based on the historical speed database. To account for the error in estimating the downstream spot speed, the upper and lower bound of v_i^D are provided by the following equations:

$$v_{ub}^D = \sigma_{ub} \times V_{hist}^D\left(t^{'}\right) \times \frac{v_i^U}{V^U} \tag{5.6}$$

$$v_{lb}^D = \sigma_{lb} \times V_{hist}^D\left(t^{'}\right) \times \frac{v_i^U}{V^U} \tag{5.7}$$

where v_{ub}^D and v_{lb}^D are respectively the upper and lower bound of the vehicle at the downstream detector; V^U is the current average speed of the upstream detector; $\sigma_{ub} \geq 1$ and $\sigma_{lb} \leq 1$ are respectively the associated upper and lower bound factors; V_{hist}^D is the historical average speed of the downstream detector at time $t^{'}$. The time $t^{'}$ is chosen such that it is matched with the arrival time, which is estimated by a linear speed profile of the modeled section, at the downstream detector. The estimation of downstream spot speeds can be viewed as a prediction-correction process. First, the historical average speed $V_{hist}^D\left(t^{'}\right)$ is adopted to predict the speed of this vehicle at downstream site. Then, this prediction is corrected by the factor v_i^U / V^U for the better representation of the current traffic condition. Finally, the upper and lower bound factors (σ_{ub} and

σ_{lb}) are applied for determining the upper and lower bound of the downstream spot speed. With the estimated downstream speeds, the corresponding upper and lower bound of the arrival time (i.e. arrival time window) of vehicle U_i can be calculated as follows:

$$Ub_i = t_i^U + \frac{l}{0.5\left(v_i^U + v_{lb}^D\right)} \tag{5.8}$$

$$Lb_i = t_i^U + \frac{l}{0.5\left(v_i^U + v_{ub}^D\right)} \tag{5.9}$$

However, it should be noted that the proposed VRI-based incident detection system is not confined to the above method for estimating the arrival time window. Any other estimation methods are equally applicable to the proposed system. With the estimated arrival time windows, vehicles on the monitored expressway section could be "partially" tracked and re-identified in a timely and accurate manner. Therefore, the incident detection time could be reduced.

5.5 Vision-based vehicle re-identification

As explained previously, the proposed VRI system is devised based on the video image data provided by the traffic surveillance cameras. By applying myriad image processing techniques, the detailed vehicle feature data (e.g. color, type and length) could be obtained. The vehicle matching process is then performed by comparing these vehicle feature data across the consecutive detectors. In this section, the methodologies involved in the VRI system are presented.

5.5.1 Vehicle re-identification problem

For a vehicle D_k arrives at downstream station at time t_k^D, the vehicle signature, denoted as $X_k^D = \{C_k^D, S_k^D, L_k^D\}$, is then obtained from the VIPs (see Section 5.2.2). A search space, $\mathcal{S}(k)$, which represents the potential matches at upstream station for vehicle D_k, is determined based on the calculated arrival time window. Specifically, $\mathcal{S}(k)$ is given by:

$$\mathcal{S}(k) = \left\{ U_i \in U \,\middle|\, Lb_i \le t_k^D \le Ub_i \right\} \tag{5.10}$$

where U_i represents the vehicle detected at upstream station; $[Lb_i, Ub_i]$ is the associated arrival time window. The vehicle re-identification problem is to find the corresponding upstream vehicle for D_k through the search space $\mathcal{S}(k)$. Herein we introduce the assignment function μ to represent the matching result:

$$\mu(k):\begin{cases} D_k \rightarrow \{U_i \in \mathcal{S}(k) | i=1,2,\cdots N\} \\ k \mapsto i, \quad i=1,2,\cdots,N \end{cases} \tag{5.11}$$

in which $\mu(k)=i$ indicates that vehicle D_k is the same as U_i. Recall that for each vehicle $U_i \in \mathcal{S}(k)$, one may assign to the pair of signatures (X_i^U, X_k^D) the distance $\{d_{color}(i,k), d_{type}(i,k), d_{length}(i,k)\}$ based on Equation 5.2, 5.3 and 5.4. In this case, one simple method (i.e. distance-based method) is to find the matched upstream vehicle with the minimum feature distance. However, it should be noted that the vehicle signatures derived from VIPs contain potential noise and are not unique. Therefore the distance measure cannot really reflect the similarities between the vehicles.

Instead of directly comparing the feature distances, this study utilizes the statistical matching method. Based on the calculated the feature distances $\{d_{color}(i,k), d_{type}(i,k), d_{length}(i,k)\}$, a matching probability $P(\mu(k)=i \mid d_{color}, d_{type}, d_{length})$ between vehicles U_i and D_k is provided for the matching decision making.

5.5.2 Calculation of matching probability

The matching probability, also referred to as the *posterior* probability, plays a fundamental role in the proposed VRI system. By applying the Bayesian rule, we have

$$P(\mu(k)=i \mid d_{color}, d_{type}, d_{length}) = \frac{p(d_{color}, d_{type}, d_{length} | \mu(k)=i) P(\mu(k)=i)}{p(d_{color}, d_{type}, d_{length})} \tag{5.12}$$

in which $p(d_{color}, d_{type}, d_{length} | \mu(k)=i)$ is the likelihood function; $P(\mu(k)=i)$ is the prior knowledge of the assignment function. In addition, we also have:

$$p(d_{color}, d_{type}, d_{length}) = p(d_{color}, d_{type}, d_{length} | \mu(k)=i) + p(d_{color}, d_{type}, d_{length} | \mu(k) \neq i) \tag{5.13}$$

Based on Equation 5.12 and 5.13, it is easy to observe that the calculation of the matching probability is dependent on the likelihood function and the prior probability. In this particular case, the prior probability is defined as $P(\mu(k)=i)=0.5$. The calculation of the likelihood function is completed in two steps. First, individual statistical models for the three feature distances are constructed and the corresponding likelihood functions are also obtained (i.e. $p(d_{color} | \mu(k))$,

$p(d_{type}|\mu(k))$ and $p(d_{length}|\mu(k))$). Then, a data fusion rule is employed to provide an overall likelihood function used in the *posterior* probability (Equation 5.12).

Statistical Modelling of Feature Distance

Without loss of generality, only the probabilistic modeling of color feature distance is described. In the framework of statistical modeling, the distance measure is assumed to be a random variable. Thus, for a pair of color feature vectors (C_i^U, C_k^D), the distance $d_{color}(i,k)$ follows a certain statistical distribution. The conditional probability (i.e. likelihood function) of $d_{color}(i,k)$ is then given by:

$$p\left(d_{color}(i,k)\,|\,\mu(k)\right)=\begin{cases} p_1(d_{color}(i,k)) & \text{if} \quad \mu(k)=i \\ p_2(d_{color}(i,k)) & \text{if} \quad \mu(i)\neq i \end{cases} \tag{5.14}$$

where p_1 denotes the probability density functions (pdf) of distance $d_{color}(i,k)$ when color feature vectors C_i^U and C_k^D belong to the same vehicle, while p_2 is the pdf of the distance $d_{color}(i,k)$ between different vehicles. A historical training dataset that contains a number of correctly matched vehicle pairs is utilized for estimating the pdfs p_1 and p_2 (Sumalee and Wang, 2012). Likewise, the likelihood function for the type and length distance can also be obtained in a similar manner.

Data Fusion Rule

In this study, the logarithmic opinion pool (LOGP) approach is employed to fuse the individual likelihood function. The LOGP is evaluated as a weighted product of the probabilities and the fusion equation is given by:

$$p\left(d_{color},d_{type},d_{length}|\mu(k)\right)=p\left(d_{color}|\mu(k)\right)^{\alpha}\,p\left(d_{type}|\mu(k)\right)^{\beta}\,p\left(d_{length}|\mu(k)\right)^{\gamma}, \quad \alpha+\beta+\gamma=1 \tag{5.15}$$

in which the fusion weights, α, β and γ are used to indicate the degree of contribution of each likelihood function. The weights will also be calibrated from the training dataset.

By substituting Equation 5.13, 5.14 and 5.15 into Equation 5.12, the desired matching probability for each pair of vehicles (U_i, D_k) could be obtained. For the sake of simplicity, let P_{ik} denote the matching probability between the vehicle U_i and D_k. In this case, we may obtain a set of probabilistic measures $\{P_{ik}|i=1,2\cdots,N\}$ to represent the likelihood of a correct match between D_k and the vehicle in the search space $\mathcal{S}(k)$. The final matching decision will base on these matching probabilities and the ratio method discussed in the following subsection.

5.5.3 Ratio method for final matching decision

An intuitive decision-making process (i.e. the greedy method) is to sort the matches via the matching probability $\{P_{ik}|i=1,2\cdots,N\}$ and choose the vehicle U_i with the largest matching likelihood:

$$\mu(k)=i, \quad \text{if } P_{ik} \le P_{jk} \ \ \forall j \in \{1,2\cdots,N\} \tag{5.16}$$

However, it is noteworthy that as the proposed VRI system is utilized for incident detection purpose, the final matching decision would produce significant impacts on the performance of the VRI-based incident detection system. Based on the greedy method (Equation 5.16), the potential false alarms would be triggered easily. As shown in Figure 5.3, the downstream vehicle D_k arrives at the time 10:39:39 AM. U_j and U_i are respectively the two candidate vehicles with the largest and the second largest matching probabilities with the downstream vehicle D_k (i.e. $P_{jk}=0.9295$ and $P_{ik}=0.8392$). Although vehicle D_k actually matches with vehicle U_i (based on manual matching), the greedy method yields the matching result $\mu(k)$=j, which could lead to a false alarm at time Ub_i.

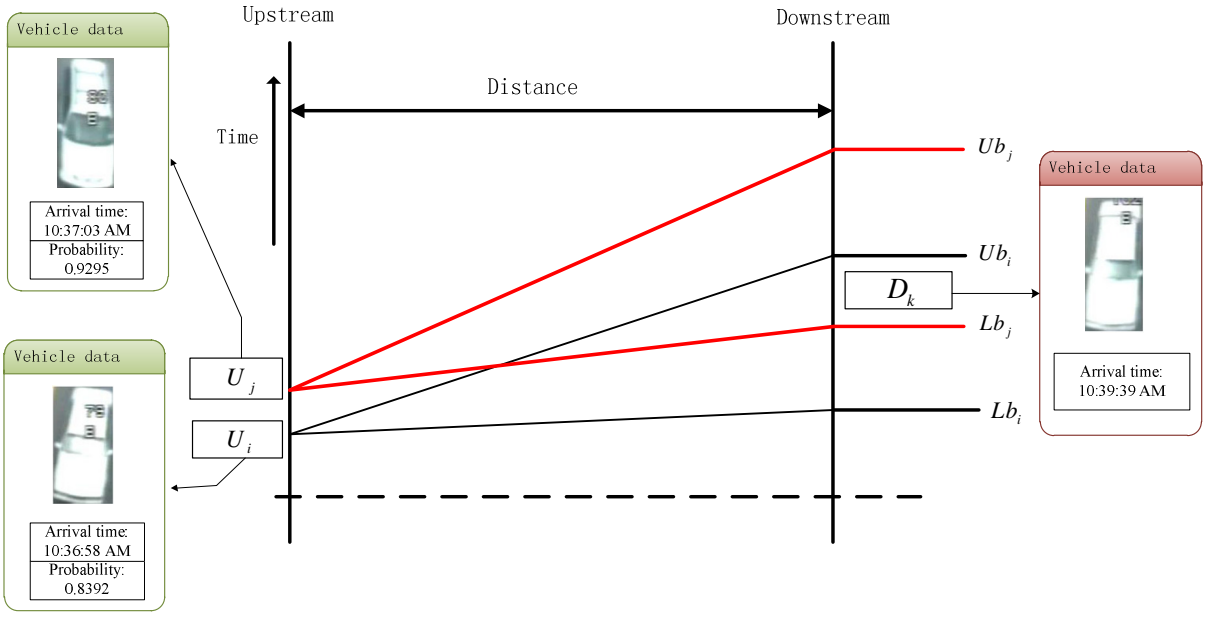

Figure 5.3 Illustrative example of a false alarm.

To reduce the false alarms mentioned above, a ratio method is then introduced for the final matching decision. Let $\{P_i|i=1,2,\cdots N\}$ denote the ordered set of matching probabilities, in which P_1 is the largest one. The ratio method proposed in this study involves two major steps. First, by imposing a threshold δ on the value of the ratio between the neighboring probabilities in the

ordered set $\{P_i | i=1,2,\cdots N\}$, one may be able screen through the search space and rule out those unlikely matches (i.e. with extremely low matching probability). The screening procedure is described as follows:

1. Set $i=1$.
2. At step i, the ratio of P_i to P_{i+1} is compared to the threshold δ. If $(P_i/P_{i+1})>\delta$, then $\{i+1,i+2,\cdots N\}$ is the unlikely match set and stop. Otherwise, set $i=i+1$ and repeat step 2

The underlying implication of this screening process is that if the ratio (i.e. P_i/P_{i+1}) is sufficiently large, then it could come to a conclusion that vehicles $\{i+1,i+2,\cdots N\}$ are the unlikely matches. Otherwise, if the ratio $P_i/P_{i+1} \le \delta$, then we may declare that vehicles i and $i+1$ are not distinctive from each other and a matching decision cannot be made at current step.

Upon the completion of the above screening process, unlikely matches will be ruled out and the search space is further reduced. The second step is then to make a matching decision based on the remaining search space $\mathcal{S}_R(k)$. Let $\mathcal{S}_R(k)=\{U_m | m=1,2\cdots M\}$, the matching result is then given by:

$$\mu^*(k)=m, \quad \text{if } Ub_\ell \ge Ub_m \ \forall \ell \in \{1,2\cdots,M\} \tag{5.17}$$

It is obvious that vehicle D_k is matched to the vehicle in $\mathcal{S}_R(k)$ with the smallest upper bound in the predicted arrival time window. The rationale behind this approach is that a matching decision could not be made based on the matching probabilities. In this case, the vehicle D_k is matched to the upstream vehicle with smallest upper bound in the predicted arrival time window to avoid the potential false alarms.

5.6 Summary

In this section, a modified vision-based VRI system is proposed to partially track the individual vehicle for identifying the “missing” vehicle due to an incident. The proposed VRI-based incident detection system is developed based on the intrinsic vehicle features (e.g. color, length and type) extracted from the videos. A flexible arrival time window is estimated for each of the individual vehicle at upstream station to improve the matching accuracy. To reduce the potential false alarms, a screening method, which is based on the ratios of the matching probabilities and arrival time windows, is introduced to rule out the potential mismatches.

CHAPTER 6 Test results for incident detection algorithms

In this chapter, the proposed TP-based incident detection algorithm (Chapter 4) and VRI-based incident detection algorithm (Chapter 5) are tested with the extracted incident data (Section 3.2.3). The three TP-based incident detection algorithms (California algorithm, McMaster algorithm and Rule-based McMaster algorithm) are implemented and compared in Section 6.1. In Section 6.2, the VRI-based incident detection algorithm will be tested with simulated and real-world case studies.

6.1 Traffic parameter-based incident detection algorithm

In this section, the performance of the California algorithm, McMaster algorithm and Rule-based McMaster algorithm are compared in terms of detection rate, false alarm rate and median time to detect. The algorithms are tested with the 36 congestion-induced incidents on Kanchanapisek Expressway (Table 3.2) with the corresponding traffic parameters (e.g. flows, occupancies) collected from the traffic sensors. Also, outputs of the three algorithms within a chosen day are compared and discussed in Section 6.1.4.

6.1.1 California algorithm

As discussed in the Section 4.2, the thresholds for the California algorithm (i.e. T_1, T_2, and T_3) are obtained by maximizing the Composite index (CI, defined in Equation 4.2) that depends on the extracted occupancies and incident data. The calibration results and corresponding performance indices for the California algorithm on each of the sections are shown in Table 6.1. From this table, it could be seen that the detection rates are less than 50 percent on 8 out of 10 sections. Thus, in terms of detection rate, the California algorithm performed poorly in most sections. Despite the poor performance in detection rate, the false alarm rates are acceptable (i.e. less than 0.1%) in all sections with a maximum FAR of 0.09% at section 10. For the median time to detect, the California algorithm could, on average, detect an incident in 18 minutes and with the longest detection time of 48 minutes in section 4. The poor detection rates and median time to detect of the California algorithm highlight the limitation of the adjacent sensors algorithms (i.e. the California algorithm) on long span detection sections such as the Karnchanapisek Expressway route. Therefore, single station algorithms (e.g. McMaster algorithm) are implemented and tested in the next subsections.

Table 6.1 Parameters for California algorithm and performance indices

Section	Real Incident Cases	T_1	T_2	T_3	DR	FAR	MTTD (min)
1	2	-45.8629	-102.7987	5.8606	0.0%	NA	NA
2	8	25.5539	-108.0327	2.9268	25.0%	0.040%	3.5
3	1	-72.4694	-55.5402	4.6376	0.0%	NA	NA
4	7	-27.8764	-76.8056	22.4277	14.3%	0.000%	48
5	3	22.0961	-37.1209	2.8672	33.3%	0.010%	31
6	3	-47.6881	-26.4899	13.1426	33.3%	0.000%	20
7	2	38.3699	-56.2917	7.1281	50.0%	0.000%	17
8	3	20.5834	-46.9809	4.1742	100.0%	0.050%	12
9	2	-73.5532	-35.7663	4.876	50.0%	0.000%	2
10	5	15.1123	-60.4259	0.85741	100.0%	0.090%	8

6.1.2 Mcmaster algorithm

In this study, the key parameters of the McMaster algorithm ($OCMAX$, $Vcrit$ and $g(OCC)$) are obtained from the flow-occupancy plots of the 10 expressway sections. The maximum uncongested occupancy ($OCMAX$) and minimum discharge volume ($Vcrit$) are respectively taken as 25% and 30 veh/hr for all road sections in this study. The minimum uncongested volume threshold is defined as following function:

$$g(OCC)=1.2*OCC$$

The performance indices of the calibrated McMaster algorithm for the 10 expressway sections are reported in Table 6.2. In this table, it could be observed that the detection rate (DR) of the McMaster algorithm has been significantly improved as compared to the California algorithm. In the McMaster algorithm, the 7 out of 10 section have a 100% detection rate while section 10 has a minimum detection rate of 80%. For the false alarm rate, the McMaster algorithm is inferior to the California algorithm. The 9 out of 10 sections have a FAR larger than 0.1% with section 5 has the maximum FAR of 1.65%. The median time to detect of the McMaster algorithm performs slightly better than the California algorithm with an average of 13.5 minutes. In order to maintain the high detection rate and to improve the false alarm rate of the McMaster algorithm, the Rule-based McMaster algorithm, which is proposed in Section 4.4, is implemented and test in the next section.

Table 6.2 Performance indices for McMaster algorithm and Rule-based McMaster algorithm

Section	Real Incident Cases	McMaster Algorithm			Rule-Based McMaster Algorithm			
		DR	FAR	MTTD (min)	T_a	DR	FAR	MTTD (min)
1	2	100.0%	0.440%	6	0.30	100.0%	0.000%	7
2	8	87.5%	1.400%	9	0.30	87.5%	1.020%	15
3	1	100.0%	0.240%	15	0.05	100.0%	0.230%	15
4	7	85.7%	0.200%	8.5	0.95	100.0%	0.130%	9
5	3	100.0%	1.650%	20	0.30	100.0%	0.400%	2
6	3	100.0%	0.170%	26	0.30	100.0%	0.080%	16
7	2	100.0%	0.120%	27.5	0.30	100.0%	0.080%	11
8	3	100.0%	0.340%	8	0.05	100.0%	0.320%	8
9	2	100.0%	0.020%	6.5	0.00	100.0%	0.020%	6.5
10	5	80.0%	0.250%	8.5	0.30	100.0%	0.120%	8

6.1.3 Rule-based McMaster algorithm

As mentioned in Section 4.4, the implementation/calibration of the Rule-based McMaster algorithm is consists of two steps: i) determination of the Rule-Based Confident Index (RCI), and ii) determination of the adaptive threshold (T_a). Based on the 2,074 time slots with detected incidents, the RCI for each of the combination of traffic states is calculated (Column 5 of Table 6.3). Among the four combinations, combination 3 (upstream state = 3 and downstream state = 1) has the highest RCI of 1.000 while combination 2 (upstream state = 2 and downstream state = 1) has the lowest value of 0.002. The estimated RCIs will then be used in the determination of T_a and algorithm implementation.

Table 6.3 McMaster's traffic states and Rule-Based Confidence Index (RCI)

Combination No.	Upstream Traffic State	Downstream Traffic State	Time slots with detected incident	RCI
1	2	1	464	0.293
2	2	2	3	0.002
3	3	1	1,586	1.000
4	3	2	21	0.012
		Total	2,074	-----

As discussed in the Section 4.4, the adaptive thresholds for the Rule-based McMaster algorithm are obtained by maximizing the Composite index (CI) that defined in Equation 4.2. The estimated section-specific threshold values, T_a, is shown in the 6th column of Table 6.2 and are ranged from 0 to 0.95 depending on the traffic characteristics on each section. In terms of detection rate the Rule-

based McMaster algorithm performs better than the McMaster algorithm with 9 out of 10 section have a 100% detection rate. Despite not all the FAR is less than 0.1%, all the FARs in this Rule-based McMaster algorithm are improved as compare to the McMaster algorithm. For individual section, the Rule-based algorithm have different performance on median time to detect as compared to the McMaster algorithm: Sections 5, 6, 7, and 10 received a shorter detection time of up to 18 minutes, and sections 1, 2, and 4 received a longer detection time from 1 to 6 minutes. On average, the median time to detect of the Rule-based McMaster algorithm (9.75 minutes) outperforms the McMaster algorithm.

6.1.4 Comparison of algorithms

Figure 6.1a, 6.1b and 6.1c respectively shows the occupancy, volume and speed of section number 2 of the studied expressway on Monday, March 26, 2012. Similar to the previous figures, the blue circles represent the data from the upstream detector stations (3A4A) while the red crosses are from the downstream (5A6A). From Table 3.2, there is an incident occurred between 14:10 and 19:20 on this section of road. As discussed in the previous section, the occupancies (speeds) at the upstream detector will increase (drop) during the incident period (Figure 6.1a and 6.1c). Figure 6.1d shows the incident alarm for the real situation (green) and the three incident detection algorithm: California algorithm (blue), McMaster algorithm (brown) and Rule-based McMaster algorithm (orange). Comparing the results of California algorithm with the McMaster algorithm in the incident period (14:10~19:20), it could be seen that the McMaster algorithm have a longer period of time with an incident alarm. This agrees with the observation in Section 6.1.1 and 6.1.2 that the McMaster algorithm has a higher detection rate than the California algorithm. Considering the results of McMaster algorithm in the period 02:00 ~ 05:00, a large number of incident alarms are issue despite there is no incident (check the case of real situation in Figure 6.1d). Such false alarms do not appear in the California algorithm and Rule-based McMaster algorithm. To sum up, the Rule-based McMaster algorithm, which has a higher detection rate than the California algorithm and lower false alarm rate than the McMaster algorithm, have the best performance in incident detection.

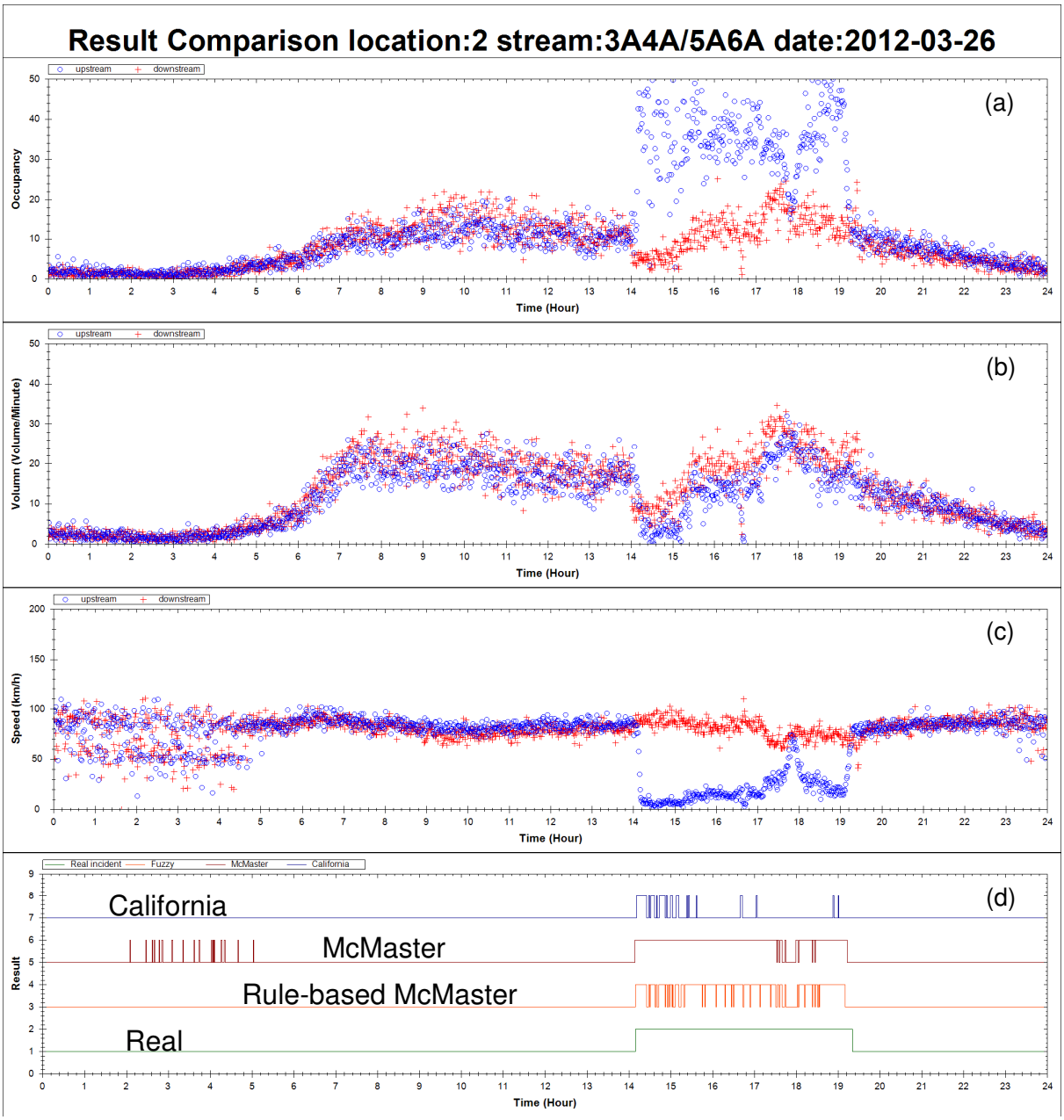

Figure 6.1 Traffic characteristics and the comparison of algorithms

6.2 Vehicle reidentification-based incident detection algorithm

In this section, the performance of the proposed VRI-based incident detection algorithm is evaluated against the classical vehicle count approach in terms of mean time-to-detect and false alarm rate (i.e. false alarms per hour). As the performance of the proposed algorithm relies on its two critical components, flexible time window estimation and vision-based vehicle re-identification method, different sizes of time window and thresholds for final matching decision are tested in this section. The dataset described in Section 5.2.2 are used to perform the simulated tests for the algorithm evaluation. Also, two real-world case studies are carried out in this section.

6.2.1 Simulated tests

For calibrating and testing the proposed VRI-based incident detection algorithm, the 3,682 pairs of vehicle matching results from the collected dataset are divided into two parts. First, a dataset of 800 pairs of correctly matched vehicles are used for the model calibration and training. The upper and lower bound factors for time window estimation (i.e. σ_{ub} and σ_{lb}) are calibrated by using the travel time data of the 800 vehicles and the historical average speeds on Thursday, which is the same as the test day (i.e. 16/2/2012, 23/2/2012, 1/3/2012 and 8/3/2012). In addition, the parameters of the statistical model (i.e. p_1 and p_2) are estimated by utilizing the feature data extracted from the captured images of these 800 pairs of vehicles. Second, the remaining 2,828 pairs of vehicles detected at both upstream and downstream detectors are fed into the calibrated VRI-based incident detection system for model evaluation. In order to mimic an incident between the upstream and downstream detector, the record of vehicle at downstream site is intentionally removed to simulate the situation that vehicle has passed the upstream detector but not the downstream one. In the testing of the proposed system, the VRI-based incident detection algorithm (Chapter 5) is run for 2,828 times, which for each run one record of the 2,828 vehicle at the downstream detector is removed, for determining the mean detection time.

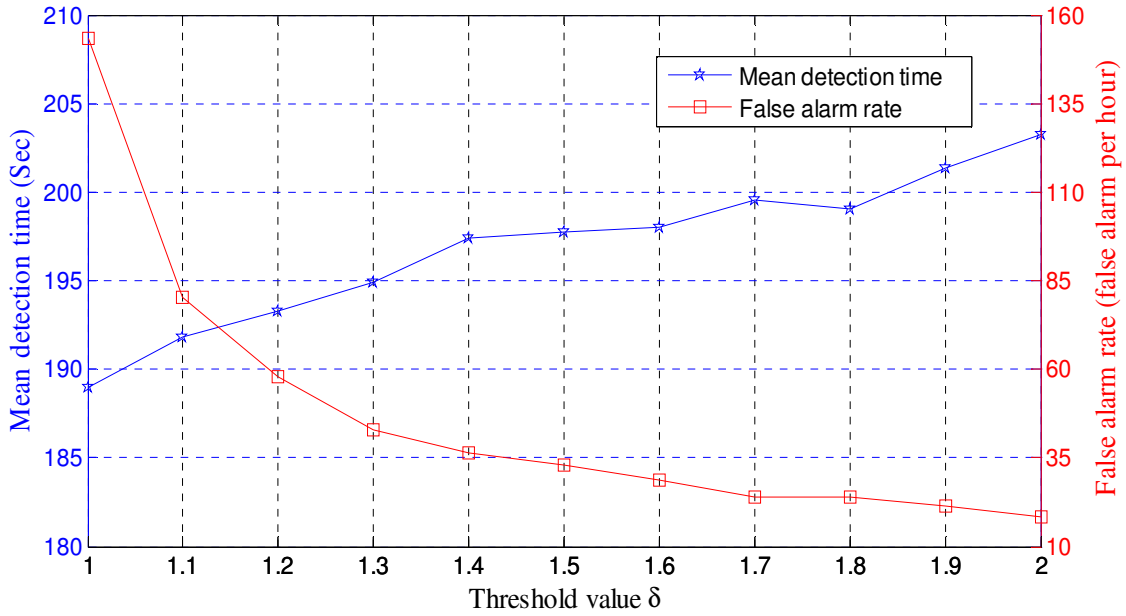

Figure 6.2 Mean detection time and false alarm rate.

By setting the threshold value equals to 2 (i.e. δ=2), the mean detection time of the proposed AID algorithm is 203.2 seconds, whereas the mean detection time of the classical vehicle count approach is 644.1 seconds. As it is expected, the mean detection time is reduced substantially by incorporating the vision-based vehicle re-identification. Figure 6.2 shows the performance of the VRI-based incident detection algorithm for different threshold values adopted in final matching

decision (Section 5.5.3). It could be observed that the false alarm rate reduces as the threshold value increases. When the threshold value equals to 1, the VRI-based incident detection algorithm will always match the downstream vehicle to the upstream one with the largest matching probability. Therefore, it would lead a large number of false alarms (see Section 5.5.3). With the increase in threshold value, the VRI-based incident detection algorithm is more relied on the traditional vehicle count approach, and resulted in a decrease in the false alarm rate. On the other hand, as the proposed VRI system is more relied to the traditional vehicle count approach (e.g. $\delta \to \infty$), the mean detection time also increases (see Section 5.3.1). To sum up, for the proposed VRI-based incident detection algorithm, the lowering of false alarm rates is at the expense of incident detection time. Thus, a balance should be struck between the rapid incident detection and low false alarm rate.

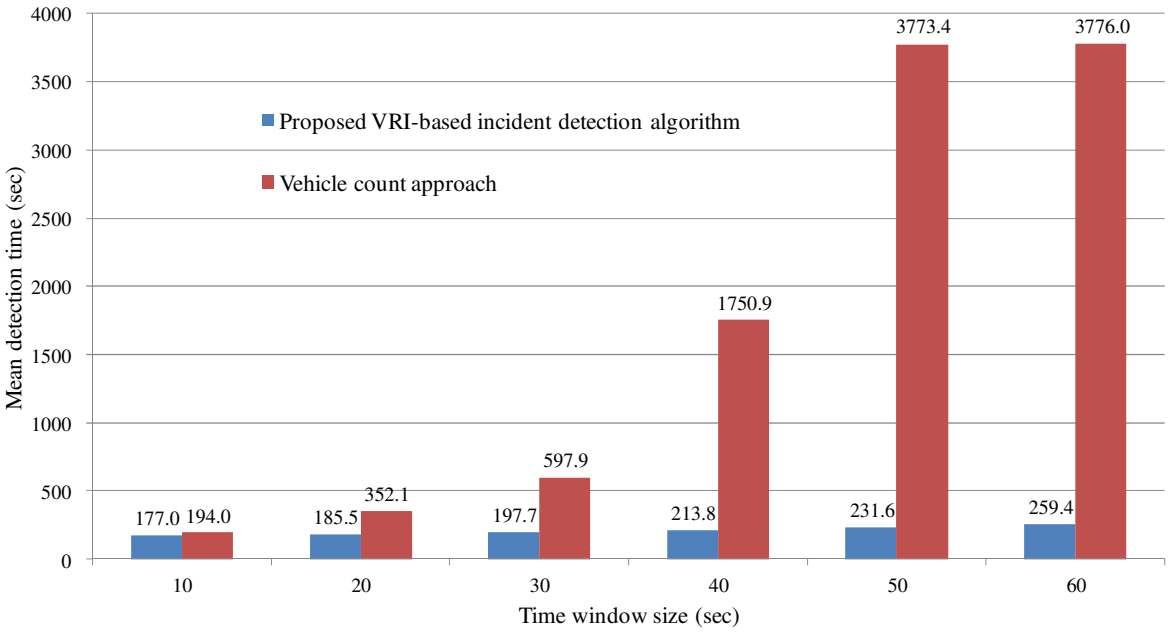

Figure 6.3 Comparison between the proposed AID algorithm and vehicle count approach.

The estimation of arrival time window also has a significant impact on the performance of the proposed VRI-based incident detection algorithm. It is not difficult to understand that a smaller time window size would result in faster incident detection. To test the performance of the proposed algorithm under different time window sizes, time window with fixed size is assigned for each individual vehicle. Figure 6.3 shows the mean detection times of the algorithms for different time window sizes. The mean detection time of the vehicle count approach increases dramatically as the size of time window grows. It is also observed that the vehicle count approach is not able to detect the missing vehicle as the size of time window is larger than 50 seconds. To sum up, for the situation that a large arrival time window is required, which either the estimation of arrival time is not accurate or a low false alarm rate is required, the proposed VRI-based incident detection algorithm clearly outperforms the vehicle count approach.

6.2.2 Real-world case studies

Apart from the abovementioned simulated tests, two real-world case studies are also carried out. Based on the incident report from the expressway authority, an incident is reported on 13-Jun-2012 at 16:03. The reported incident location is at 20+600 westbound, which is in the section 4 (see Figure 3.1 and Table 3.1) of the Kanchanapisek expressway. Based on this information, the research team has screen through the captured videos for identifying the incident vehicle. It is found out that on 13-Jun-2012, the incident vehicle has passed the upstream detector (7A/8A) at 15:55 (Figure 6.4a) and has an incident before it reaches the downstream detector (9A/10A). 4 minutes later, a tow-truck, which is probably called by the driver of the incident vehicle, has passed the upstream detector (Figure 6.4b) and towed the incident vehicle to pass the downstream detector at 16:09 (Figure 6.4c).

(a) (b) (c)

Figure 6.4(a) Incident vehicle passes the upstream detector; (b) Tow truck passes the upstream detector; (c) Incident vehicle and tow truck passes through the downstream detector. (For incident on 13-June-2012)

According to the above information of the incident vehicle, a 35-minutes video record data (from 15:33 to 16:08 on 13-Jun-2012) of location 8A and 10A are extracted and input into the proposed VRI-based incident detection system. In this case, apart from the incident vehicle, 739 vehicles are detected at both stations during the 35-minutes video record. By setting the threshold value of the ratio of matching probabilities equals to 8.5, the time of incident detection and the false alarm rate for this case study are found to be 15:58:22 and 3.42 false alarms per hour respectively. Compared with the classical vehicle count approach, which would trigger an incident alarm at 16:01:28, the proposed AID system performs better in terms of the incident detection time.

(a) (b)

Figure 6.5(a) Incident vehicle passes the upstream detector; (b) Incident vehicle and tow truck passes through the downstream detector. (For incident on 17-June-2012)

The second case study is based on the incident report on 17-Jun-2012 at 10:31 at location 19+300 westbound. Similarly, from the captured videos, the research team found that the incident vehicle has passed the upstream detector (7A/8A) at 10:24 (Figure 6.5a). 33 minutes later, the incident vehicle, which is towed by a tow truck, has passed the downstream detector (Figure 6.5b). Based on this information, the corresponding videos from the upstream and downstream cameras are fed into the proposed VRI-based incident detection system. By setting the threshold value equals to 8.5, the time of incident detection and the false alarm rate for this case study are found to be 10:28:25 and 2 false alarms per hour. In the case study, the detection time of the proposed algorithm also outperforms the classical vehicle count approach, which will trigger an incident alarm at 10:33:50.

CHAPTER 7 Conclusions

7.1 Summary

In congested urban road network, one minor traffic incident could result in gridlocks and severe congestion problems. In order to efficiently and effectively handle traffic incidents for avoiding such adverse impacts, incident detection is the first and crucial step to be considered by system operators and traffic engineers. Thus, this project aims to develop an automatic expressway incident detection system for addressing this issue. In this project, traffic parameter-based (TP-based) and vehicle reidentification-based (VRI-based) incident detection algorithm have been proposed for detecting incidents in different traffic conditions. The TP-based algorithm will mainly be used for detecting the congestion-induced incidents of which the occurrence of incidents will have substantial impacts to the traffic conditions (e.g. flow, occupancy, etc) detected by traffic sensors. On the other hand, the VRI-based algorithm will mainly be used in the non-congested, or free-flow, traffic conditions such that the occurrence of incidents will not induce any congestions/delays that could be detected by the traffic sensors. The proposed models/algorithm will be calibrated and test with the traffic (e.g. occupancy) and video data collected from the traffic sensors on a 24-km section of the Kanchanapisek expressway.

In this project three different TP-based incident detection algorithms have been introduced and tested: California algorithm, McMaster algorithm and Rule-based McMaster algorithm. California algorithm detects an incident by considering the temporal and/or spatial changes of occupancies. McMaster algorithm detects an incident by considering the traffic states, which is defined by the occupancies and flows, at the upstream and downstream ends of the section. Rule-based McMaster algorithm extends the McMaster algorithm by introducing a Rule-Based Confident Index in incident detection. Composite Index, which is the combination of the three commonly used indices (detection rate, false alarm rate and mean time to detect), is proposed for calibrating the proposed algorithms with the collected incident and traffic data. The calibrated TP-based algorithms are then compared in terms of detection rate, false alarm rate and median time to detect for incident detection on different sections of the studied expressway. In this study it is found out that the detection rates of the two single station approaches (McMaster algorithm and Rule-based McMaster algorithm) are higher than that for the California algorithm. This result could be explained by the deficiency of the adjacent sensor algorithm (California algorithm) for detecting incidents on long spans (5 km). In terms of false alarm rate and median time to detect, the Rule-based McMaster algorithm outperforms the McMaster algorithm. To sum up, the Rule-based McMaster algorithm has the best performance among the three tested TP-based algorithms for detecting incidents on the Kanchanapisek expressway.

In this project, a vision-based system, which depends on the video records collected at the detector stations, is proposed for the VRI-based incident detection algorithm. In the proposed algorithm, each individual vehicle is identified (i.e. extracting vehicle features) and re-identified (i.e. matching the extracted vehicle features) at different detector stations. Incident is then detected by identifying the missing vehicle in between the detectors of a close expressway corridor/system. In this study, image segmentation technique is adopted for capturing the still images of vehicles from the videos fed into the system. Then, these captured images are analyzed for extracting the vehicle features: color, length and type. Based on the extracted vehicle features, data fusion techniques (LOGP approach) and Bayesian rule are proposed for determining the matching probability of the captured upstream and downstream vehicles. Flexible time window estimation is proposed in this study for improving the matching accuracy. To reduce the potential false alarms, a screening method, which is based on the ratios of the matching probabilities and arrival time windows, is introduced to rule out the potential mismatches. The developed VRI-based incident detection algorithm is calibrated and tested on a 3.6-kilometer segment of the Kanchanapisek expressway. Simulated and real-world case studies have been completed for testing the performance of the proposed algorithm. In the simulated case studies, it is found that the false alarm rate (mean detection time) decreases (increases) as the threshold in the ratio method, which is proposed for the screening of potential mismatches, increases. Both of the simulated and real-world case studies show that the proposed VRI-based incident detection algorithm has a shorter detection time as compared to the traditional vehicle count approach.

7.2 Further research

For the developed automatic expressway incident detection system in this project, there are several directions of future research. First, an in-depth analysis of the performance of TP-based and VRI-based incident detection algorithm under different traffic conditions will be completed. Based on the understanding of performances, the fusion model could be enhanced for the better use of the incident detection results from these two algorithms. Second, more incident data will be collected to recalibrate the TP-based incident detection algorithm(s) for shortening the detection time. Third, efficient matching algorithm will be developed for the case of multiple entrances/exits in the VRI-based incident detection algorithm. This matching algorithm is crucial for extending the proposed VRI-based incident detection algorithm to the network case. Lastly, focuses will also put on enhancing the current video image processing system/algorithm to handle detection errors from the traffic surveillance systems.

References

Balke, K.N. (1993) An evaluation of existing incident detection algorithms. Federal Highway Administration (FHWA/TX-93/1232-20).

Balke, K., Chaudhary, N., Chu, C., Kunchangi, S., Nelson, P., Songchitruksa, P., Sunkari, S., Swaroop, D. and Tyagi, V. (2007) Dynamic Traffic Flow Modeling for Incident Detection and Short-Term Congestion Prediction. Austin: Federal Highway Administration.

Bhattacharyya, A. (1943) On a measure of divergence between two statistical populations defined by their probability distributions. Bulletin of the Calcutta Mathematical Society, 35, 99-109.

Chang, S.L., Chen, L.S., Chung, Y.C. and Chen, S.W. (2004) Automatic license plate recognition. IEEE Transactions on Intelligent Transportation Systems, 5, 42-53.

Chang, G., and Su, C.-C. (1995) Predicting intersection queue with neural network models. Transportation Research Part C, 3(3), 175-191.

Chen, S. and Wang, W. (2009) Decision tree learning for freeway automatic incident detection. Expert System with Application, 36, 4101-4105.

Coifman, B. (1998) Vehicle Re-Identification and Travel Time Measurement in Real-Time on Freeways Using Existing Loop Detector Infrastructure. Transportation Research Record, 1643, 181-191.

Coifman, B., and Cassidy, M. (2002) Vehicle reidentification and travel time measurement on congested freeways. Transportation Research Part A, 36(10), 899-917.

Coifman, B. and Krishnamurthy, S. (2007) Vehicle reidentification and travel time measurement across freeway junctions using the existing detector infrastructure. Transportation Research Part C, 15(3), 135-153.

Dipti, S., Xin, J. and Long, C.R. (2004) Evaluation of Adaptive Neural Network Models for Freeway Incident Detection. IEEE Transactions on Intelligent Transportation Systems, 5(1), 1-11.

Fambro, D.B. and Ritch, G.P. (1980) Evaluation of an algorithm for detecting urban freeway incidents during low-volume conditions. Transportation Research Record, 773, 31-39.

Forbes, G. J. (1992) Identifying Incident Congestion. Institute of Transportation Engineers, 62, 17-22.

Google Maps. (2012) Map of Bangkok Expressway [Online]. Mountain View, California: Google Inc. Available: www.maps.google.com [Accessed July 28, 2012].

Guin, A. (2004) An Incident Detection Algorithm Based On a Discrete State Propagation Model of Traffic Flow. Ph.D. Thesis, Georgia Institute of Technology.

Hall, F.L., Shi, Y. and Atala, G. (1993) On-line Testing of the McMaster Incident Detection Algorithm Under Recurrent Congestion. Transportation Research Record, 1394, 1-7.

Lam. W.H.K. (2008) Short-term forecasting of travel times for Hong Kong incident management. Proceedings of the ITS Hong Kong Forum 2008 – Incident Management System (IMS) Technologies and Applications, 24 September 2008, Hong Kong, 35-50.

Lee, J.-T. and Taylor, W.C. (1999) Application of a Dynamic Model for Arterial Street Incident Detection. Journal of Intelligent Transportation Systems, 5, 53-70.

Levin, M. and Krause, G.M. (1978) Incident Detection: A Bayesian Approach. Transportation Research Record, 682, 52-58.

Mahmassani, H. S., Haas, C., Zhou, S. and Peterman, J. (1995) Evaluation of incident detection methodologies. Texas Department of Transportation (FHWA/TX-00/1795-1).

Martin, P.T., Perrin, J. and Hansen, B. (2001) Incident Detection Algorithm Evaluation. Utah Department of Transportation (MPC-01-122).

Ozbay, K. and Kachroo, P. (1999) Incident Management in Intelligent Transportation Systems, Artech House, Boston, London.

Ozbay, K., Xiao, W., Jaiswal, G. and Bartin, B. (2005) Evaluation of Incident Management Strategies. Federal Highway Administration, FHWA-NJ-2005-020.

Parkany, E. and Xie, C. (2005) A complete review of incident detection algorithms & their deployment: what works and what doesn't. The New England Transportation Consortium (NETCR 37).

Payne, H.J. and Tignor, S.C. (1978) Freeway Incident-Detection Algorithms Based on Decision Trees with States. Transportation Research Record**,** 682, 30-37.

Payne, H.J. and Thompson, S.M. (1997) Development and Testing of Operational Incident Detection Algorithms: Technical Report. Federal Highway Administration, ITS Research Division, Turner-Fairbank Highway Research Center.

Persaud, B. N. and Hall, F. L. (1989) Catastrophe theory and patterns in 30-second freeway traffic data – Implications for incident detection. Transportation Research Part A*,* 23**,** 103-113.

Quayle, S.M., Koonce, P., DePencier, D. and Bullock, D.M. (2010) Arterial Performance Measures with Media Access Control Readers. Transportation Research Record, 2192, 185-193.

Shehata, M.S., Cai, J., Badawy, W.M., Burr, T.W., Pervez, M.S., Johannesson, R.J. and Radmanesh, A. (2008) Video-Based Automatic Incident Detection for Smart Roads: The Outdoor Environmental Challenges Regarding False Alarms. IEEE Transactions on Intelligent Transportation Systems, 9(2), 349-360.

Sheu, J., Lan, L. and Huang, Y. (2009) Short-term prediction of traffic dynamics with real-time recurrent learning algorithms. Transportmetrica, 5(1), 59-83.

Stephanedes, Y.J. and Chassiakos, A.P. (1993a) Application of Filtering Techniques for Incident Detection. Journal of Transportation Engineering, 119, pp. 13-26.

Stephanedes, Y.J. and Chassiakos, A.P. (1993b) Freeway incident detection through filtering. Transportation Research Part C: Emerging Technologies, 1, pp. 219-233.

Sumalee, A. and Wang, J. (2012) Probabilistic fusion of vehicle features for re-identification and travel time estimation using video image data. Transportation Research Record, accepted.

Sun, C., Ritchie, S. G., Tsai, W. and Jayakrishnan, R. (1999) Use of vehicle signature analysis and lexicographic optimization for vehicle reidentification on freeways. Transportation Research Part C, 7, 167-185.

Wang, J., Wang J., Lu, F., Cao, Z., Liao, Y. and Deng, Y. (2009) Comparison study on classification performance for short-term urban traffic flow condition using decision tree

algorithms. Proceeding of the 2009 WRI World Congress on Software Engineering, 4, 434-438.

Weil, R., Wootton, J. and García-Ortiz, A. (1998) Traffic incident detection: Sensors and algorithms. Mathematical and Computer Modelling, 27, 257-291.

Willsky, A., Chow, E., Gershwin, S., Greene, C., Houpt, P. and Kurkjian, A. (1980) Dynamic Model-Based Techniques for the Detection of Incidents on Freeways. IEEE Transactions on Automatic Control, 25, 347-360.

Wu, B.F., C.C Kao, C.C. Liu, C.J. Fan, and C.J. Chen (2008) The vision-based vehicle detection and incident detection system in Hsueh-Shan tunnel. Presented at Industrial Electronics, 2008. IEEE International Symposium on 2008.

Zhang, K. and Taylor, M.A.P. (2006) Effective Arterial Road Incident Detection: A Bayesian Network Based Algorithm. Transportation Research Part C, 14(6), 403–417.

Final Report

Research Grant 2011

ATRANS